2009-01-01

Discrete Element Modelling Of Silicon Nitride Ceramics: Crack Formation And Propagation In Indentation Test And Four Point Bending Test

Rajeev Senapati
University of Texas at El Paso, rsenapati@miners.utep.edu

DISCRETE ELEMENT MODELLING OF SILICON NITRIDE CERAMICS: CRACK FORMATION AND PROPAGATION IN INDENTATION TEST AND FOUR POINT BENDING TEST

RAJEEV SENAPATI

Department of Industrial Engineering

APPROVED:

Jianmei Zhang, Ph.D., Chair

Tzu-Liang (Bill) Tseng, Ph.D.

Wei Qian, Ph. D.

Patricia D. Witherspoon, Ph.D.
Dean of the Graduate School

Dedication

This thesis is dedicated to my parents and to all my family members and friends who supported me in every step of my life.

DISCRETE ELEMENT MODELLING OF SILICON NITRIDE CERAMICS: CRACK FORMATION AND PROPAGATION IN INDENTATION TEST AND FOUR POINT BENDING TEST

by

RAJEEV SENAPATI, B.E

THESIS

Presented to the Faculty of the Graduate School of

The University of Texas at El Paso

in Partial Fulfillment

of the Requirements

for the Degree of

MASTER OF SCIENCE

Department of Industrial Engineering

THE UNIVERSITY OF TEXAS AT EL PASO

December 2009

Acknowledgements

I want to express my deepest appreciation to Dr. Jianmei Zhang for her consistent support and guidance through the course of my graduate study and in my research. It would have been impossible to complete this work without her support. I am thankful to Dr. Zhang for teaching me the basics of research. I am thankful to my committee members – Dr. Tzu-Liang (Bill) Tseng and Dr. Wei Qian for their help. I would like to thank all the faculty members of Industrial Engineering for helping me successfully complete my Masters. I would like to thank Dr. Arunkumar Pennathur for all his support, motivations and valuable suggestion and comments. I would like to thank Dr. Rafael S. Gutierrez (Chair, Industrial Engineering) for his support.

Abstract

Advanced ceramic materials have been extensively used in aerospace, automobile and other industries. However, the reliability of the advanced ceramics is the major concern because of the brittle nature of the materials. This work aims to model silicon nitride ceramics using Discrete Element Method (DEM) and simulating the crack formation and propagation. DEM software package PFC^{2D} is used to simulate indentation test and four point bending test on silicon nitride ceramics and the behaviour of crack formation and propagation is identified. The numerical representation of ceramic materials is done by generating a densely packed particle system using the specimen genesis procedure and then applying the suitable microparameters to the particle system. Indentation test has been performed on the sample with different loading forces and the width and depth of cracks generated have been studied. Four point bending test has been simulated and the fracture origins has been identified. Simulation of four point bending test is performed on sample having no defects, sample having manufacturing-induced defects like cracks, and sample having material-inherent flaws like voids. For the above cases the initiation and propagation of defects is simulated and the mean contact force on the loading ball is also obtained and plotted. The simulation prediction results are well in accordance with the experimental nondestructive testing results.

Table of Contents

List of Figures

List of Tables

Chapter 1: Introduction

Advanced ceramics are supposed to be more beneficial than many metals in engineering applications because of their material properties like lower density, good shock resistance, higher hardness, lighter weight, superior strength at higher temperatures, higher wear and corrosion resistance, lower thermal expansion and good chemical resistance [1]. Due to these properties ceramics can provide a robust solution for many engineering application. During these days silicon nitride ceramics are being used for many engineering purposes like making blades of turbine, engine components, bearings for high speed spindles, cutting tools, welding jigs and fixtures, welding nozzles etc. Ceramics if used in manufacturing engine components can improve fuel economy, reduce emission and extend component life. Ceramic bearings have less friction and therefore, less heat loss in comparison to metal bearings [2]. Ceramics are also being used in aerospace industry due to their advantageous physical properties [3].

Due to growing industrial demand of ceramics and need for good machining accuracy and better surface finish of the ceramics, many machining technologies have been developed. Experimental researches have been done to study the machining processes on ceramics like grinding [4 – 6], scratching test [7 – 9] and single point diamond turning [10 – 12]. Other than these experimental researches many theoretical and numerical methods have been developed such as continuum damage mechanics [13] and finite element method [14].

During various machining processes of ceramics, sub-surface damage like micro-cracks are caused. It is very difficult to experimentally measure the formation of these cracks and therefore it is essential to employ a numerical simulation method to study the initiation and propagation of the cracks during machining processes in order to have a better understanding of the formation of the subsurface damage.

The micro-structure of ceramics consists of crystal particles and pores, and the ceramic materials can be treated as an assembly of discrete particles bonded together randomly and the inter granular fracture of the ceramics can be represented by the separation of the particles due to breakage of bonds. This is the concept that has been used in discrete element analysis to successfully simulate different materials like rocks [15].

1.1 Research Objective

Silicon nitride ceramics are also widely used in semiconductor industries for making Integrated Circuits (IC). These IC chips are used in critical components in machines like aircrafts, spacecrafts, earth movers etc. and the IC chips are very important for these systems. While operating, these systems generate very high vibrations which can lead to the failure of the ICs, which in turn can cause the failure of the whole system. So it is important to study the mechanical properties of silicon nitride before production of these ICs and test these ICs for any defects before they are put into use.

Among the mechanical properties, hardness is a very important property since it determines the material's resistance to shape change when force is applied. In order to determine the hardness of a material normally indentation test is performed [16 – 17]. Indentation Test can also be used to estimate surface stress [18]. Ceramics are brittle in nature and breaks easily when loaded to perform the indentation test. To prevent the ceramic from breaking, ultra-low-load indentation has to be done and such ultra-low-load indentation test makes it difficult to obtain a direct measurement of the contact area [19]. Therefore it is necessary to develop some numerical methods to simulate the indentation test.

Fracture strength is another important mechanical property which determines the maximum loading the material can withstand before fracture. Four – point bending test is used very often to test the fracture strength of a material [20 – 23].

This research aims to study these important mechanical properties of silicon nitride ceramics using the PFC^{2D} software package, and investigate crack formation and propagation in indentation test and four point bending test. The applied force is also studied.

1.2 Thesis Organization

This thesis consists of seven chapters. The first chapter gives the introduction and thesis objective; the second chapter presents some literature review; the proposed methodology – discrete element method is described in Chapter three. Simulation procedures and results of indentation test is presented in chapter four, Chapter five simulation of four point bending test. The simulation results and experimental results are discussed in the sixth chapter and conclusions and summary of contributions are drawn in chapter seven.

Chapter 2: Literature Review

2.1 Discrete Element Method (DEM)

Discrete element method was introduced by Cundall (1971) for the analysis of rock mechanics problem. Rock was represented as a dense packing of non – uniform particles that were bonded at their contact points and the mechanical behaviour was simulated using DEM [24]. DEM modelling of rock was also used to simulate a loading – type failure around an underground excavation in brittle rock. And it was shown that PFC^{2D} was capable of simulating the localization behaviour of the rock and it was able to reproduce the damage zone observed in the laboratory test using PFC^{2D} [25]. The DEM model of the rock generated by PFC^{2D} has been implemented in studying the stability of heavily joined rock slopes and also used to simulate the inelastic rock impact [26 - 27]. The behaviour of granular assemblies of elliptical particles with wide range of eccentricities has been studied by DEM [28].

DEM has also been used simulate soil mechanics, DEM model of soil has been used to study different factors of the soil and analyzing the mechanical behaviour of the soil in the presence of external forces, and the results of the DEM model were consistent with the experimental data [29]. DEM model of soil has also been used to study the interaction of soil with machines used for agricultural purposes, e.g. the interaction of cutting blade with the soil [30].

Recently, DEM has been used to measure the fracture toughness of materials. Fracture toughness of a material is the property of the material which quantifies the resistance to crack extension. DEM model was used to simulate the phenomena of fracture and the fracture toughness was measured [31].

DEM is also used to study fracture mechanics of continuous media like concrete [32] and modelling of fracture and damage in the machining process of poly crystalline SiC. DEM model of poly crystalline SiC was generated by using PFC^{2D} and the different machining process was done on the DEM model. The cracks formation and crack propagation was simulated with the help of the DEM model of SiC and it was found that the cracks formed are in accordance to the actual experimental results [33]. DEM has also been used to model thermally fractured Graphite. A numerical model of heated graphite was developed using DEM and the process of fracture in graphite due to heat was simulated. In this process not only the mechanical properties but the thermal properties were also considered. The results of the numerical method were well in accordance with the experimental results [34]. DEM assumes that a sample is made up of small discrete elements which are contained in the sample boundary. These small particles are assumed to be rigid and are in contact with other particles over a vanishingly small area. The soft – contact approach is applied at the contacts, wherein the rigid particles are allowed to overlap one another at contact points. The magnitude of overlap is small in relation to particle size and is related to contact force which is determined from the overlap and relative movements of the particle pair according to a specified force – displacement law [35].

The calculations in DEM apply Newton's second law of motion to the particles and force displacement law at the contacts. Newton's second law is applied to determine the motion of each particle and the force displacement law is applied to update the contact forces arising from the relative motion of each particle at the contacts.

2.2 Silicon – Nitride Ceramics

Pure silicon nitride is difficult to produce as a fully dense material. There are various processes which are used to fabricate silicon nitride, this fabrication methods influence the mechanical properties of the silicon nitride to a great extent. The microstructure and mechanical properties of porous silicon nitride ceramics depended mostly on the size of starting powders [36]. The three main types of silicon nitrides include Reaction bonded silicon nitride (RBSN), Hot pressed silicon nitride (HPSN) and Sintered silicon nitrides (SSN).

Reaction bonded silicon nitride (RBSN) is made by direct nitridation of a compacted silicon powder at about 1450^{o}C. During this process silicon – nitride grows in the porosity in the compact. The nitridation produces only a small volume change, and is accompanied by increase in density, which means that RBSN components do not need to be machined after fabrication and complex shapes can be produced in a single process stage. The disadvantage of this process is that the final product is highly porous and the reaction bonded silicon nitrides are less dense than hot pressed and sintered silicon nitride. Usual densities of RBSN are in the range 2300 – 2700kg.m^{-3} compared with 3000 – 3200kg.m^{-3} for hot pressed and sintered silicon nitride. The nitridation produces only a small volume change, which means that RBSN components do not need to be machined after fabrication and complex shapes can be produced in a single process stage.

Hot pressed silicon nitride (HPSN) is made by adding a flux (usually magnesia) to a fine Si_3N_4 powder and then pressing the powder in a graphite die typically at 1800°C and 40MPa of pressure. This results in production of fully dense HPSN with excellent mechanical properties. Due to its higher density HPSN materials have better physical properties and so they are used in more demanding applications. But HPSN parts tend to be expensive.

Sintered silicon nitrides (SSN) are a development on RBSN aimed at reducing the final porosity of the product and therefore improving its mechanical properties. This is achieved by adding sintering additives to the starting powder mix which allows the material to be sintered after the reaction–bonding stage. The starting raw materials for SSN principally is silicon metal. Silicon metals are relatively cheap compared to high quality silicon nitride powders and so SSN is cheaper to manufacture than both HPSN and RBSN.

Sintered silicon nitrides (SSN) are densified by pressure – less sintering in a nitrogen atmosphere at around 1750°C. In order to aid densification, various combinations of sintering additives such as yttrium oxide, magnesium oxide and aluminum oxide are used. Where there is an addition of an aluminum containing additive the sintered material can be classed as a sialon. Sialons are ceramic alloys based on the elements silicon, aluminum, oxygen and nitrogen and the term is often used interchangeably with SSN. SSN and sialon generally offer the best mechanical properties available for a silicon nitride and are the most widely used in industrial applications such as molten metal handling, industrial wear, metal forming, the oil and gas industries and the chemical and process industries.

Silicon nitride (Si3N4) has the strongest covalent bond properties next to silicon – carbide. Silicon nitride is used as a high temperature structural ceramic due to superior heat resistance, strength, and hardness. The wear and corrosion resistance in silicon nitride are excellent and so it is used in heat exchangers, vessels for chemical reactions, engines and gas turbine components [37 – 38]. Silicon nitride ceramics are widely used in optical and semiconductor industries. Silicon nitride ceramic is also used to make bearings to be used in Total hip arthroplasty (THA), and it has been mechanically tested that silicon nitride ceramic has a better fracture toughness and fracture strength over alumina ceramics [39].

There are three crystallographic structures of silicon nitride namely α, β and γ phases. The α and β phases are the most common forms of Si_3N_4, and can be produced under normal pressure condition. The γ phase can only be synthesized under high pressures and temperatures and has a hardness of 35 GPa. α phase has a trigonal structure and β phase has a hexagonal structure.

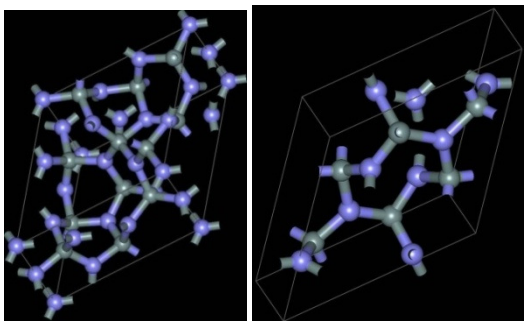

Figure 2.1: Structure of α and β silicon nitride

The important advantage of Si3N4 is the ability to tailor their microstructures and properties, by controlling the α to β phase transformation that occurs during sintering at high temperature of the mostly α phase original Si3N4 powders [40-42].

Chapter 3: Proposed Methodology

3.1 Particle Flow Code In Two Dimensions (PFC2D)

PFC^{2D} is a software package used to simulate the mechanical behavior of a system which is considered to be comprised of distinct elements. These distinct elements in the system move independently from one another and interact at the contacts. These elements are assumed to be rigid and the mechanical behavior of the system is described in terms of the movement of each element and the inter-particle forces acting at each contact point. To simulate crack formation in the system the elements are bonded together at the contact points such that when the inter-particle forces acting at any bond exceed the bond strength the bond breaks. There are two types of bonds which forms in the system, contact bonds are formed between elements which are in contact, and parallel bonds are formed between particles which are not in contact but are in close proximity.

The following are the assumptions in PFC^{2D} [35].

The particles are treated as rigid bodies.

The contact occurs at a vanishingly small area (i.e. at a point).

Behavior at the contacts uses a soft-contact approach, wherein the rigid particles are allowed to overlap one another at contact points.

The magnitude of the overlap is related to the contact force via the force-displacement law, and all overlaps are small in relation to particle size.

Bonds can exist at contacts between particles.

All particles are circular. However the clump logic supports the creation of super-particles of arbitrary shape. Each clump consists of a set of overlapping particles that act as a rigid body with a deformable boundary.

The model of the system formed by PFC^{2D} is two dimensional and consists of two-dimensional circular particles. Only two force components and one moment component exists in the PFC^{2D} model. The out of plane force component and the two in plane moment components are not considered.

The particles are considered as rigid bodies and deformation in the physical system is due to movements along the interfaces. It is assumed that the deformation results primarily from the sliding and rotation of the particles as rigid bodies and the opening and interlocking at the interfaces and not from individual particle deformation.

Other than the circular particles, the PFC^{2D} particle – flow model also includes "walls". Walls allow the user to apply velocity boundary conditions to assemblies of balls for purposes of compaction and confinement. Interaction between the particles and the walls take place due to the forces arising at the point of contact of the particles with the walls. The motion of the particles is governed by the laws of motion and each particle satisfies the laws of motion, whereas the equation of motion is not satisfied for the walls. The forces acting on the wall does not influence the motion of the wall. But the motion of the walls depends upon the parameters entered by the user. Figure 3.1 shows the sample generated in PFC^{2D}, the boundaries of the sample are denoted by the walls and the particles are denoted by the balls.

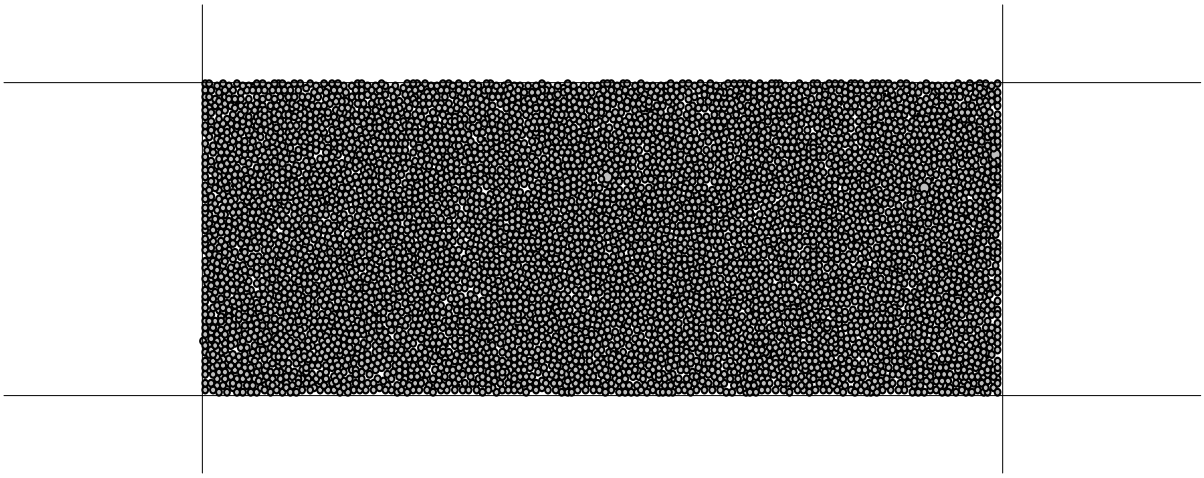

Figure 3.1: Sample generated by PFC2D.

3.2 Distinct – Element Method

Distinct – Element method (DEM) is used in PFC^{2D} to model the movement and interaction of stressed assemblies of rigid circular particles. In DEM the particle interactions are treated as dynamic process and whenever the internal forces are balanced a state of equilibrium is reached. By tracing the movements of the individual particles the contact forces and the displacements of the particles are calculated. Movement of the particles results from the disturbances caused by the walls or particle motion. This dynamic behaviour of the interaction between the particles and the interaction between the particles and the walls are represented numerically by an explicit time stepping algorithm, using a central – difference scheme to integrate accelerations and velocities. The time step chosen in DEM is so small that during a single time step, the disturbance created by a particle or a wall can only propagate to its immediate neighbors and not beyond that. Then at all times the forces acting on any particle are due to its interaction with the particles with which it is in contact.

The calculations that are performed in the DEM alternate between the applications of Newton's second of motion and a force – displacement law at the contacts. Newton's second law of motion is used to determine the motion of each particle arising from the contact and the body forces acting upon it, while the force – displacement law is used to update the contact forces arising from the relative motion at each contact.

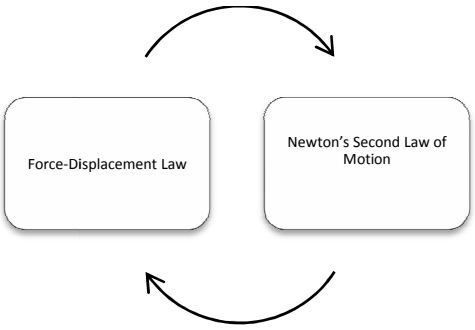

Figure 3.2: Calculation cycle in PFC^{2D}.

3.3 Bonding Models

In PFC^{2D} generated sample the particles are bonded together at contacts. There are two types of bonding models supported by PFC^{2D} the contact – bond model and the parallel – bond model. The bonds in PFC^{2D} can considered as a kind of glue joining the two particles. The contact bond is of vanishingly small size that acts only at the contact point. The contact bond can only transmit a force. The parallel bond is of a finite size that acts over either a circular or a rectangular cross-section lying between the particles, the parallel bond can transmit both a force and a moment.

3.3.1The Contact Bond Model

A contact bond can be imagined as a pair of elastic springs with constant normal and shear stiffness acting at the contact point. These two springs have specified shear and normal strengths. When there is no overlap between the particles a tensile force develops at the contact. The magnitude of the tensile normal contact force is limited by the normal contact bond strength. A contact bond is defined by two parameters they are normal contact bond strength (F^n_c) and shear contact bond strength (F^s_c). A contact bond breaks when the tensile normal contact force exceeds the normal contact bond strength as shown in Figure 3.3.

3.3.2 The Parallel Bond Model

The parallel bond can be imagined as a finite sized piece of material deposited between two particles. The two particles here are treated as spheres or cylinders. Parallel bond can transmit both forces and moments between particles.

.

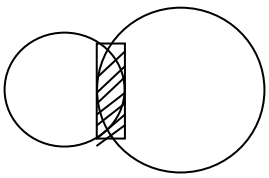

Figure 3.3: Parallel bond depicted as a finite sized piece of material.

3.4 Specimen Genesis Procedure

The specimen genesis procedure is an inbuilt function in PFC^{2D}, which is used to generate a rectangular sample of the material in PFC^{2D}. The inputs to the specimen genesis procedure are divided into two types. The first types of inputs are those inputs which control the specimen

genesis procedure and the second types are those which define the material which is being simulated.

The following four steps comprise the specimen genesis procedure:

Compact Initial Assembly: In this step a rectangular sample is generated according to the length and breadth provided to the procedure, the sides of the rectangle acts as the walls of the sample. Then this rectangle is filled with randomly generated particles of the specified size and the radius ratio. The wall normal stiffness is set to β times the average particle normal stiffness. The value of β is entered by the user according to the material. The sizes of the particles are uniformly distributed with specified values of minimum and maximum radii. To ensure a good initial packing of the particles in the sample the porosity of the sample is maintained at 16% and according to this porosity the number of particles are determined. For different random arrangements different numbers of particles are generated.

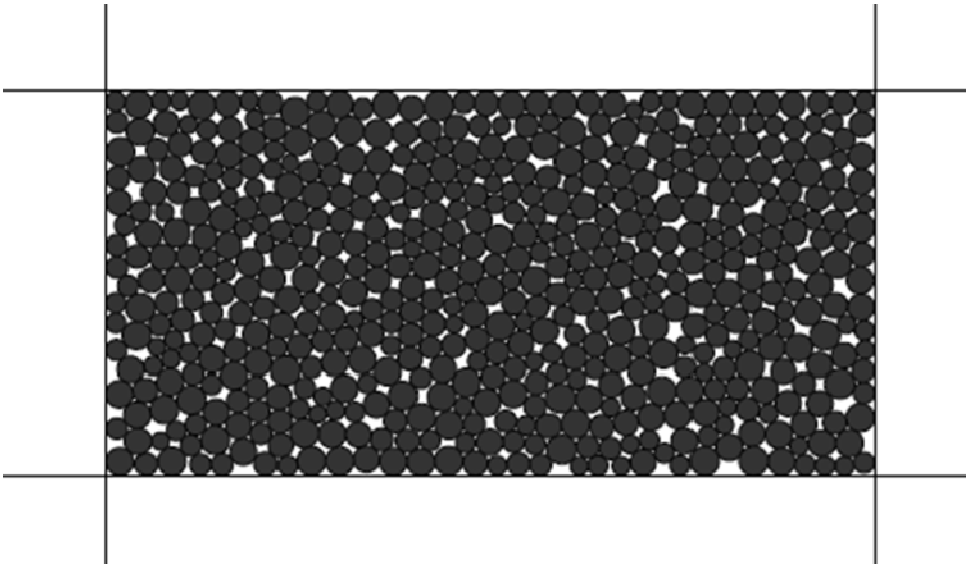

Figure 3.4: Particle assembly generated after the first step

Install Specified Isotropic Stress: In this step the radii of all the particles are changed uniformly to achieve a specified isotropic stress σ_0, isotropic stress is defined as the mean of the two direct stresses σ_x and σ_y.

Reduce The Numbers Of Floating Particles: Floating particles are those particles which have less than three contacts, in an assembly of randomly placed particles with non uniform radius there can be large number of floating particles. In order to get a denser network of bonds in the bond installation step it is required to have less number of floating particles.

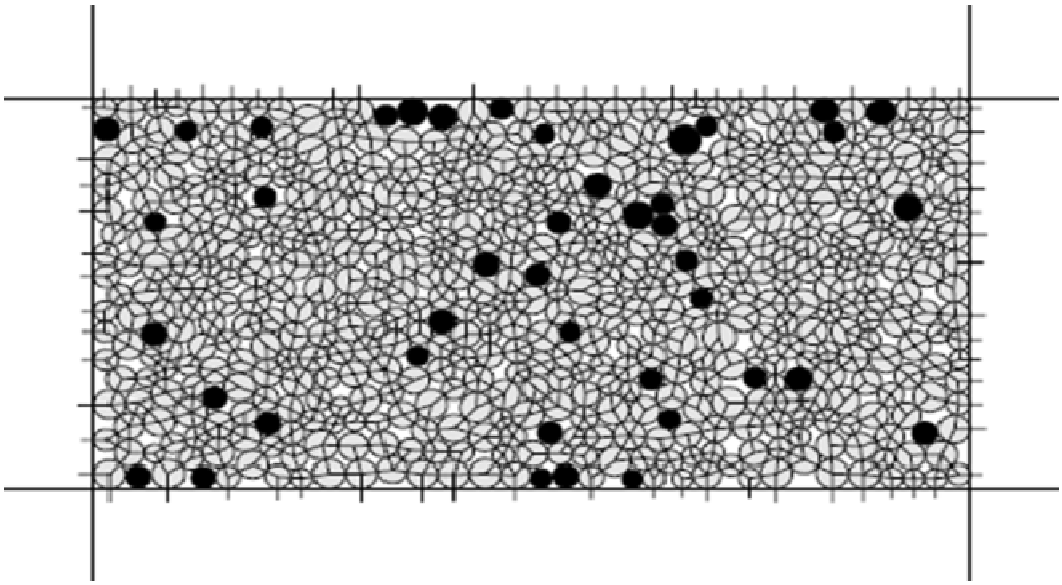

Figure 3.5: Floating Particles in a sample generated by PFC^{2D}.

Finalize Specimen: In the final step of this procedure the bonds are installed in the sample. Contact bonds are formed between particles which are in physical contact and parallel bonds are formed among particles which are not in physical contact but are in near proximity. Then all particles are assigned a friction coefficient.

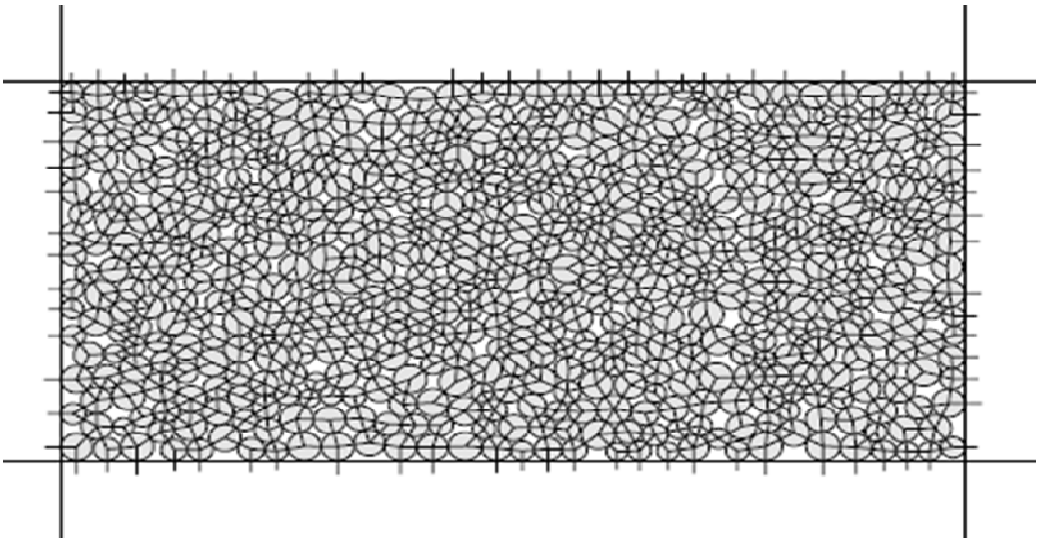

Figure 3.6: Bond network after the completion of specimen genesis procedure

Table 3.1: The parameters that controls the specimen genesis procedure

Parameters	**Symbols**
Sample height (m)	h
Sample width (m)	w
Minimum ball radius (m)	R_{min}
Ball size ratio, uniform distribution	R_{max}/R_{min}
Wall normal stiffness multiplier	β
Locked – in isotropic stress (Pa)	σ_0
Remaining floaters ratio	n_f/N

Table 3.2: The microparameters that define a parallel – bonded material

Parameters	Symbols
Ball density (kg/m^3)	ρ
Ball – ball contact modulus (Pa)	E_c
Ball stiffness ratio	k_n/k_s
Parallel – bond radius multiplier	$\overline{\lambda}$
Parallel – bond modulus (Pa)	$\overline{E_c}$
Parallel – bond stiffness ratio	$\overline{k_n}/\overline{k_s}$
Ball friction coefficient	μ
Parallel – bond normal strength, mean (Pa)	$\overline{\sigma_c}$ (mean)
Parallel – bond normal strength, std. dev. (Pa)	$\overline{\sigma_c}$ (std. dev.)
Parallel – bond shear strength, mean (Pa)	$\overline{\tau_c}$ (mean)
Parallel – bond shear strength, std. dev. (Pa)	$\overline{\tau_c}$ (std. dev.)

3.5 Biaxial And Brazilian Test Environment

After the creation of the sample by the specimen genesis procedure it is very important to test the sample to check if its physical properties are same to the material which is being simulated. To test the sample we use the biaxial and Brazilian test.

3.5.1Biaxial Test

The biaxial test begins by loading the sample. The sample is loaded by moving the upper and lower walls towards each other at some specified velocity. During subsequent loading phase the stresses and strains are computed. During the biaxial test, the deviatoric stress, $\sigma_d = \sigma_y - \sigma_x$ is monitored and the maximum value of $| \sigma_d |$ is recorded. During the test this value will initially

increase and then decrease as the sample fails, the test is terminated when $| \sigma_d | < \alpha (\sigma_d)_{max}$. The setup of the biaxial test is shown in figure 8.

The quantities that are monitored using this test are:

1. Stresses and strains.
2. Energy quantities.
3. Microcracks.

Upon completion of the biaxial test, the following sets of responses are received.

1. Poisson's ratio.
2. Young's Modulus.
3. Compressive strength.
4. Crack initiation stress.
5. The total number of normal and shear type cracks existing in the sample at peak load.

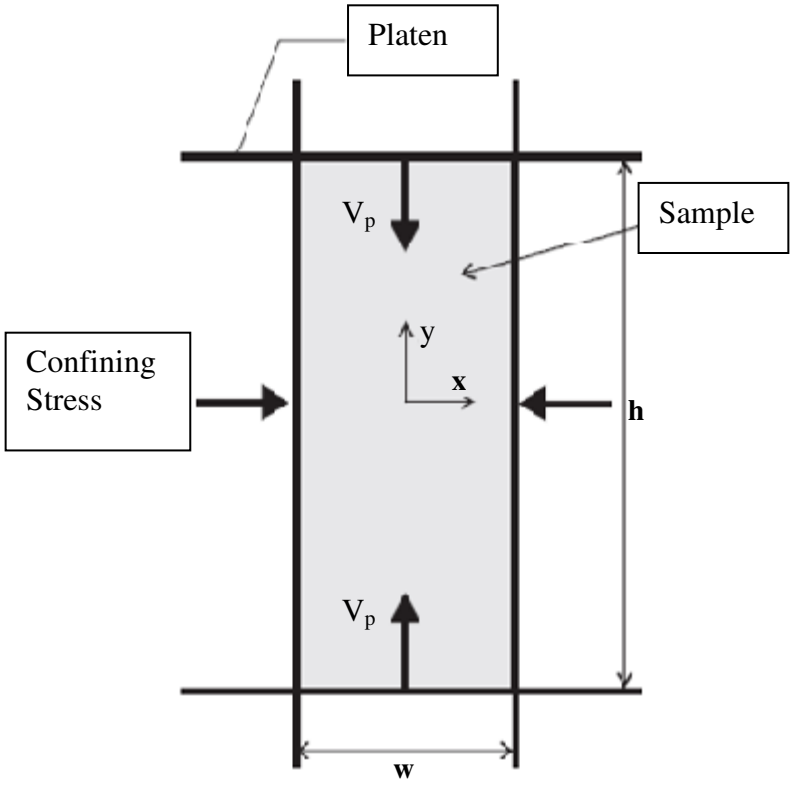

Figure 3.7: Biaxial Test

3.5.2 Brazilian Test

In the Brazilian test the sample is trimmed into a circular shape that is in contact with the lateral walls, the lateral walls are then moved towards each other with a specified velocity in steps. During this test the average force acting on the lateral walls are monitored. During the test the force will initially increase to some maximum value and then will decrease as the sample fails. The test is terminated when $F < \alpha * F_{max}$. The Brazilian test setup is shown in figure 9.

Upon completion of the Brazilian test the following set of responses are received:

1. The peak force
2. The total number of normal and shear type of cracks existing in the specimen at peak load.

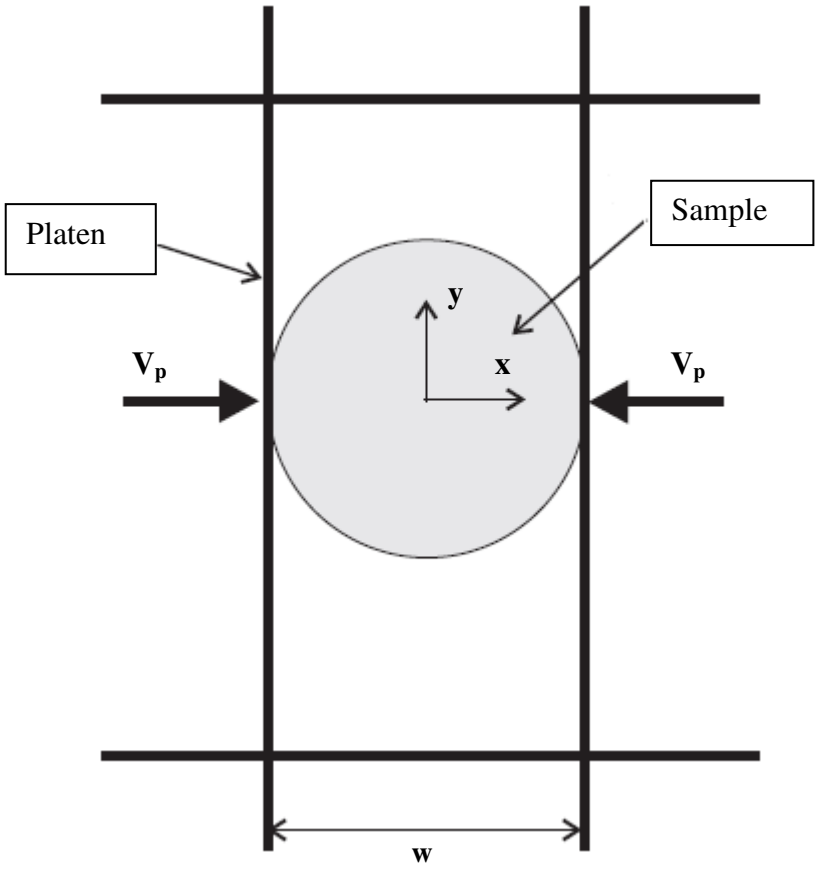

Figure 3.8: Brazilian test

Chapter 4: Indentation Test

4.1 DEM Modeling of Indentation Test

The PFC^{2D} software package has been utilized to create a DEM model for the simulation of Indentation test on silicon nitride ceramics. The specimen genesis procedure was used to generate the sample of the silicon-nitride ceramic to perform the Indentation test. The dimensions of the specimen generated used for simulation were 7 mm height and 25 mm in length. The microparameters used to generate the specimen in the PFC^{2D} are given in the Table 4.1 [43]. The sample generated has been shown in Figure 4.1. For the Indentation test the loading ball had a radius of 2.25 mm and is placed at the top of the specimen as shown in Figure 4.2. A wall was placed above the loading ball and was accelerated to simulate the force on the loading ball.

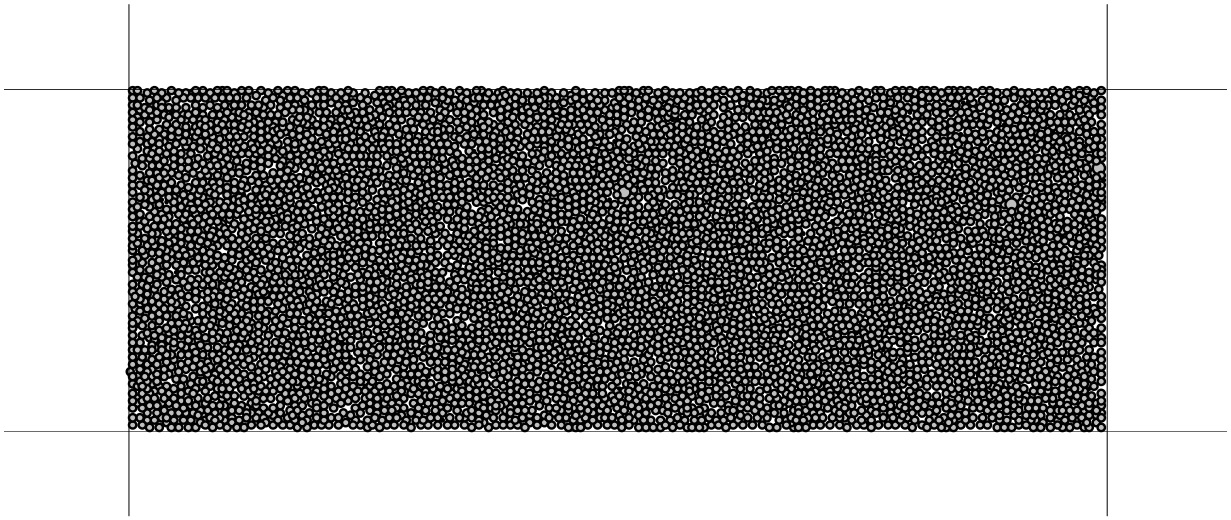

Figure 4.1: Sample generated by PFC^{2D} for indentation test

To simulate the different forces on the loading ball, the loading ball was subjected to different accelerations, and to do that the loading ball was moved in negative Y – direction from an initial zero velocity to a specified final velocity. This final velocity of the loading ball was achieved in many steps and in many cycles. Here in this simulation three different final velocities has been used to simulate different applied force, the velocities considered are 2 m/s, 3 m/s and 5 m/s.

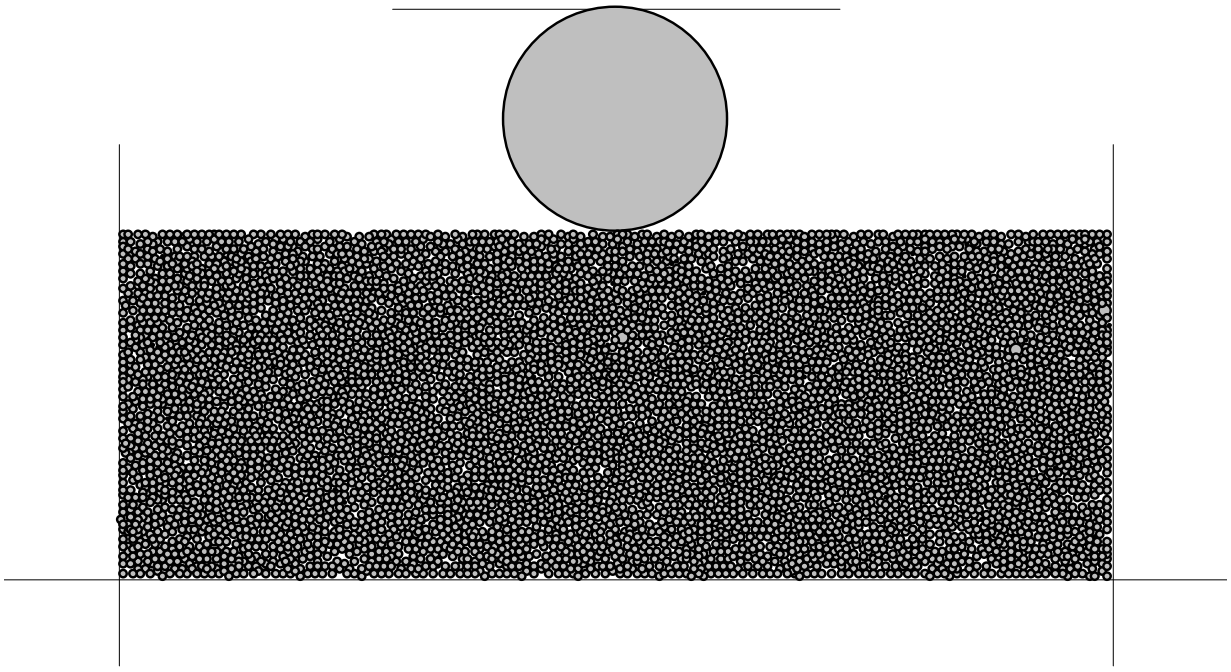

Figure 4.2: Indentation test setup.

Table 4.1: Microparameters used in the program to simulate sample for Indentation test.

Microparameters	**Values**
Density	3200 kg/m^3
Ball-Ball contact modulus	220e9 Pa
Ball Stiffness ratio (k_n/k_s)	1.3
Parallel-bond radius multiplier	1.0
Parallel-bond modulus	220e9 Pa
Parallel-bond stiffness ratio	1.3
Ball friction coefficient	0.4
Parallel-bond normal strength, mean	1400e6 Pa
Parallel-bond normal strength, std. dev	280e6 Pa
Parallel-bond shear strength, mean	1400e6 Pa
Parallel-bond shear strength, std.dev.	280e6 Pa

4.2 Results of Indentation Test

The Indentation test was performed using three different forces, which were simulated by three different final velocities and the depth and width of crack was studied. Also the force applied by the loading ball is plotted.

4.2.1 Final Velocity 2 m/s

The cracks formed when the loading ball is accelerated from zero initial velocity to final velocity of 2 m/s is shown in figure 4.3. The cracks are shown in black color. Figure 4.4 shows the corresponding force diagram.

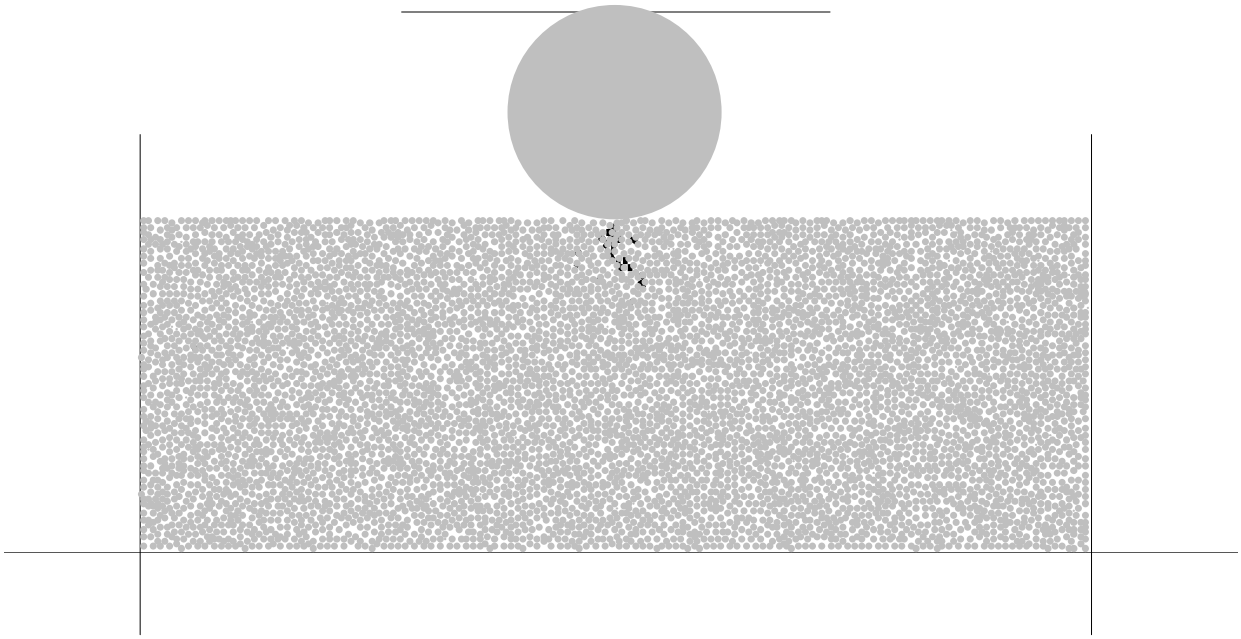

Figure 4.3: Cracks formed when the final velocity of the loading ball is set to 2 m/s.

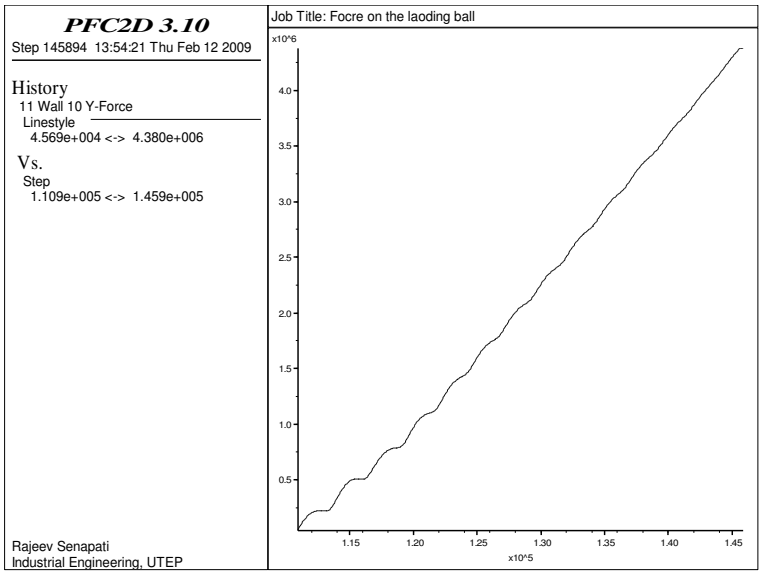

Figure 4.4: The force diagram of the indentation test, when the final velocity of the loading ball is set to 2 m/s.

4.2.2 Final velocity 3 m/s

The cracks formation in case the final velocity of the loading ball is set to 3 m/s is shown in figure 4.5. Figure 4.6 shows the corresponding force diagram.

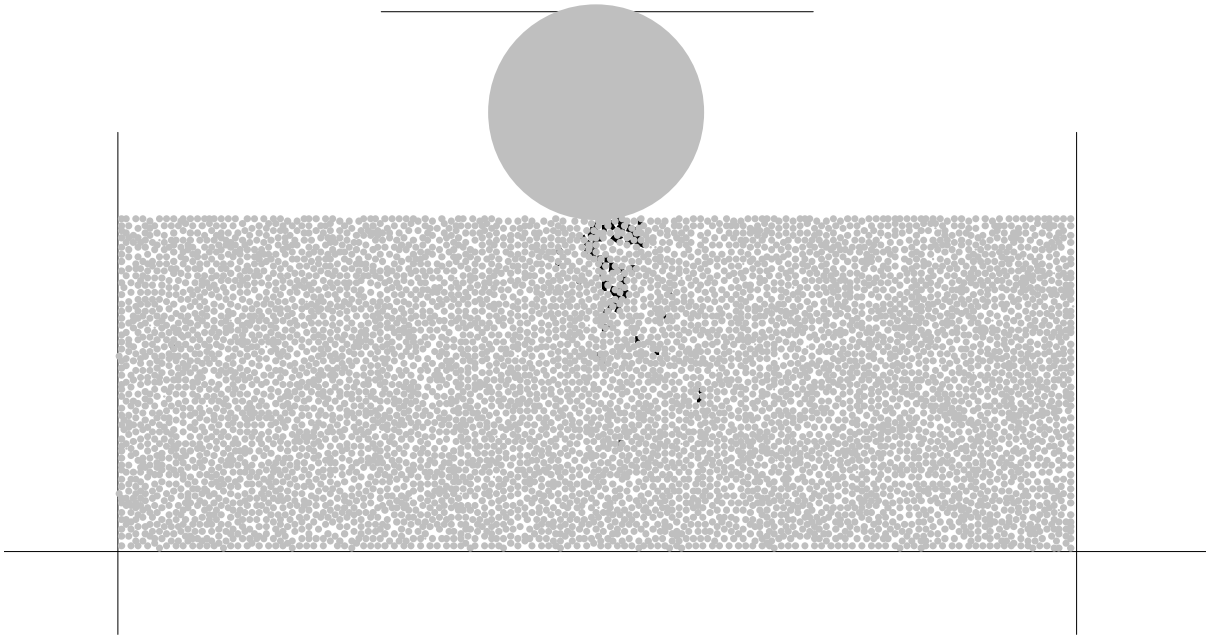

Figure 4.5: Cracks formed when the final velocity of the loading ball is set to 3 m/s.

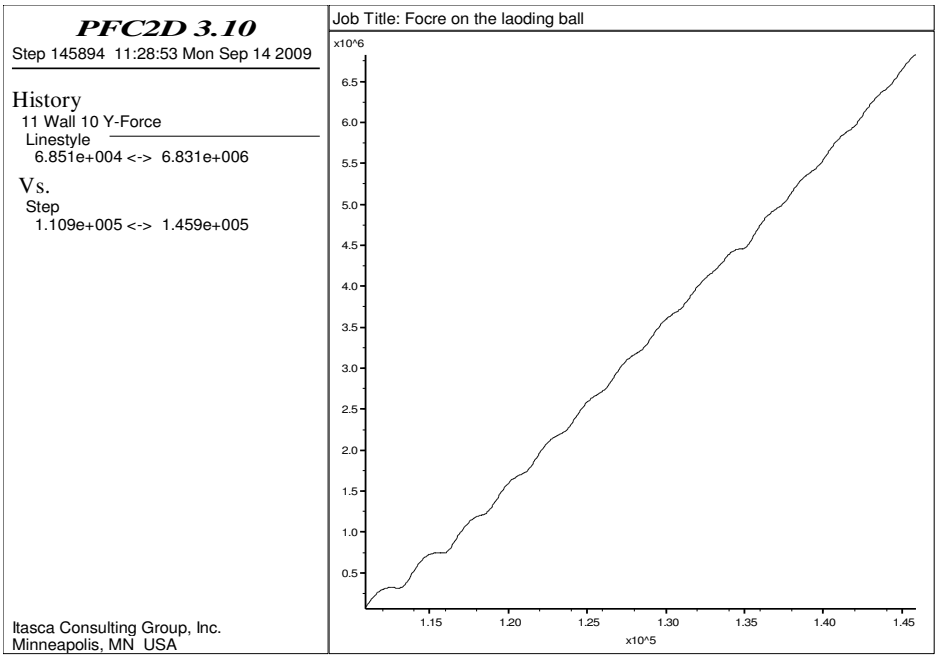

Figure 4.6: Force diagram of the indentation test, when the final velocity of loading ball is set to 3 m/s.

4.2.3 Final velocity 5 m/s

When the final velocity of the loading ball is set to 5 m/s, the crack formation which is received is shown in figure 4.7 and the corresponding force diagram is shown in figure 4.8

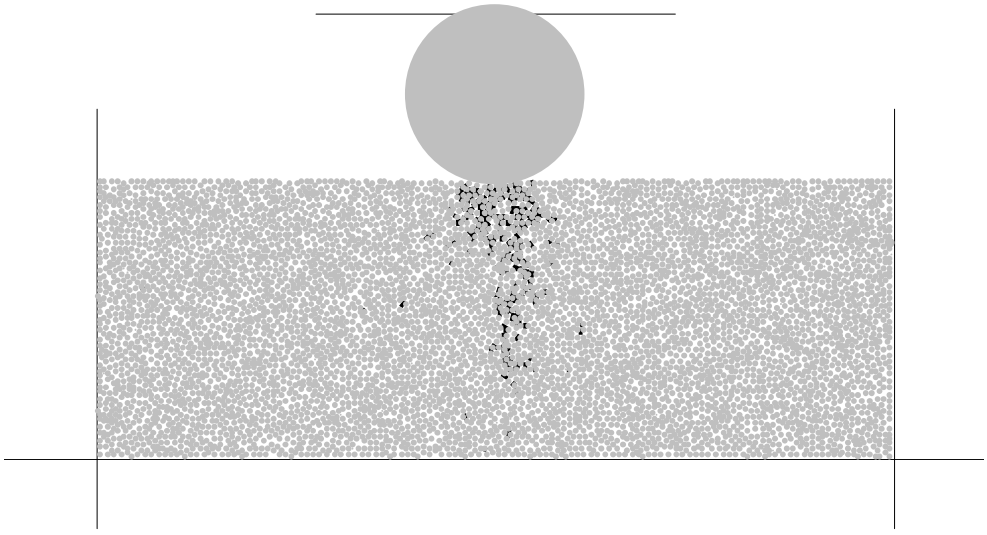

Figure 4.7: Cracks formed when the final velocity of the loading ball is set to 5 m/s.

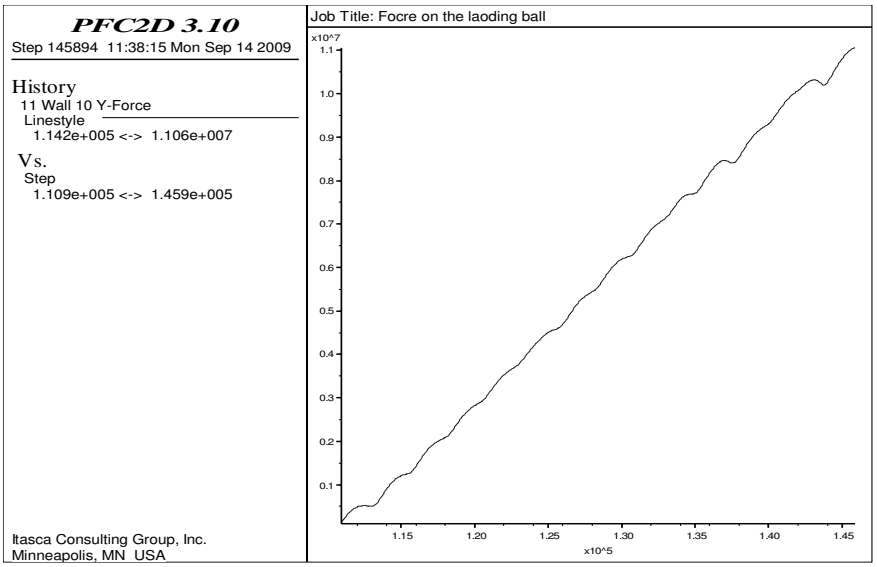

Figure 4.8: The force diagram of the indentation test, when the final velocity of the loading ball is set to 3 m/s

Chapter 5: Four-Point Bending test using PFC^{2D}

5.1 DEM Modeling of Four-Point Bending Test

The PFC^{2D} software package has been utilized to create a DEM model for the simulation of Four-Point Bending test on silicon nitride ceramics. The specimen genesis procedure was used to generate the sample of the silicon-nitride ceramic to perform the four-point bending test. The dimensions of the specimen generated used for simulation were 7 mm height and 25 mm in length. The microparameters used to generate the specimen in the PFC^{2D} are given in the Table 5.1. The sample generated has been shown in Figure 5.1. For the four-point bending test, the inner span is 10 mm and the outer span is 20 mm. The loading balls had a radius of 2.25 mm and were placed at the top of the specimen as shown in Figure 5.2. A wall was placed above the loading balls and was accelerated to simulate the force on the loading balls. Two supporting balls were placed below the sample to support the sample as another two points.

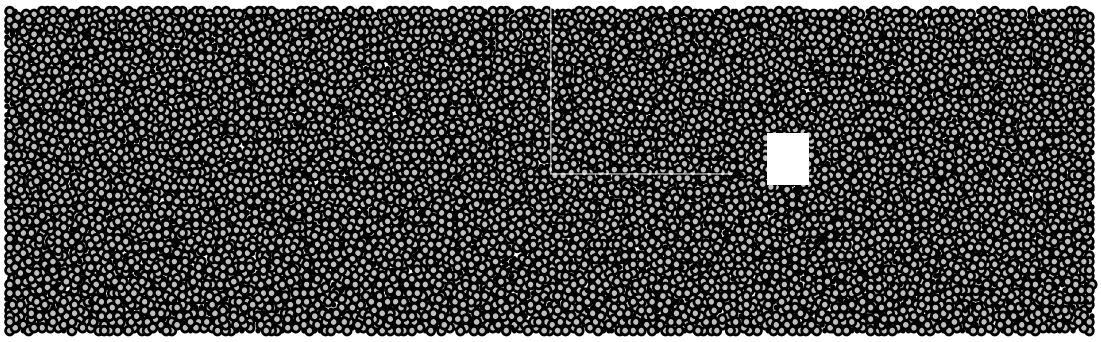

Figure 5.1: Particle assembly generated by specimen genesis procedure in PFC2D.

Table 5.1: Microparameters used in PFC2D simulation of Silicon nitride ceramics.

Microparameters	Values
Density	3200 kg/m^3
Ball-Ball contact modulus	220e9 Pa
Ball Stiffness ratio (k_n/k_s)	1.3
Parallel-bond radius multiplier	1.0
Parallel-bond modulus	220e9 Pa
Parallel-bond stiffness ratio	1.3
Ball friction coefficient	0.4
Parallel-bond normal strength, mean	1400e6 Pa
Parallel-bond normal strength, std. dev	280e6 Pa
Parallel-bond shear strength, mean	1400e6 Pa
Parallel-bond shear strength, std.dev.	280e6 Pa

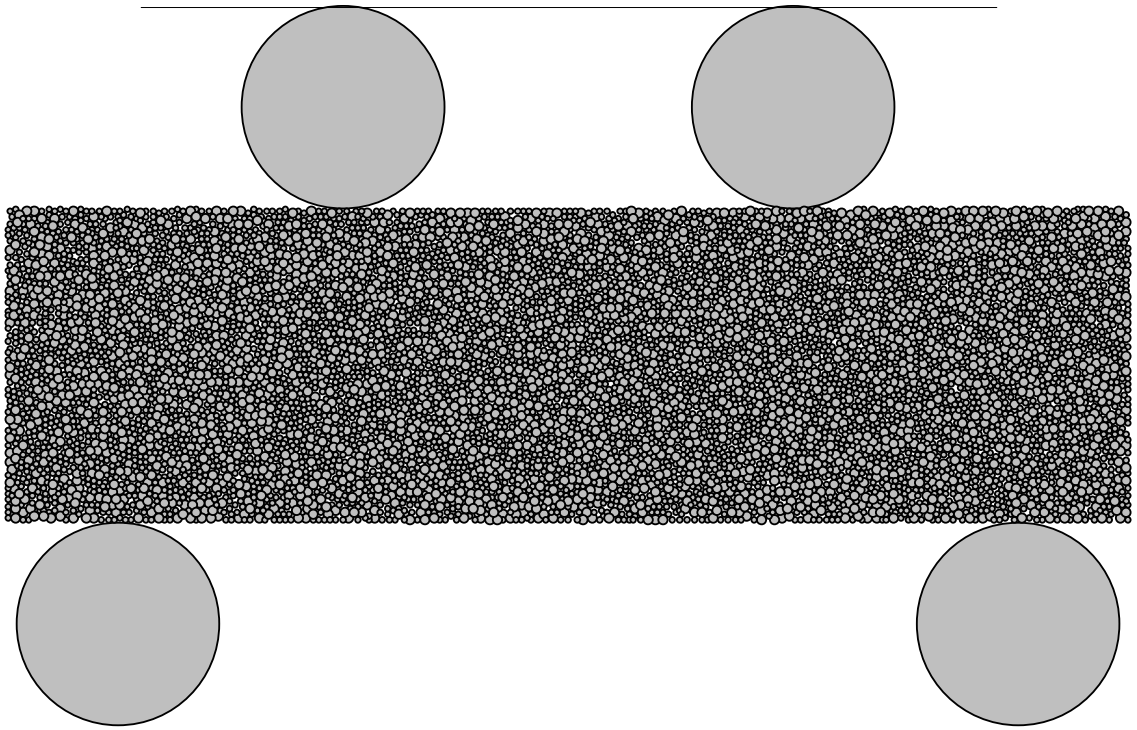

Figure 5.2: DEM modeling of four-point bending test

5.2 Results of Four-Point Bending Test Using PFC^{2D}

Based on the authors' previous work on nondestructive evaluation of silicon nitride ceramics, the fracture could start from the manufacturing-induced flaws like cracks, could start from the material-inherent flaws like voids. Therefore, the four-point bending test simulation is performed for three different cases, sample with no defects, sample with manufacturing defects, and sample with material-inherent flaws. In all the above cases the location of the fracture origin was determined and the force at the point where the sample fails is recorded.

5.2.1 Sample With No Defect

Figure 5.3 shows the fracture on the sample with no apparent manufacturing-induced defects or material-inherent flaws. A bunch of simulations have been performed for this case and it was found that the location of fracture origin could be varying if using different particle assemblies. Figure 5.4 shows the force diagram of the four-point bending test on this sample.

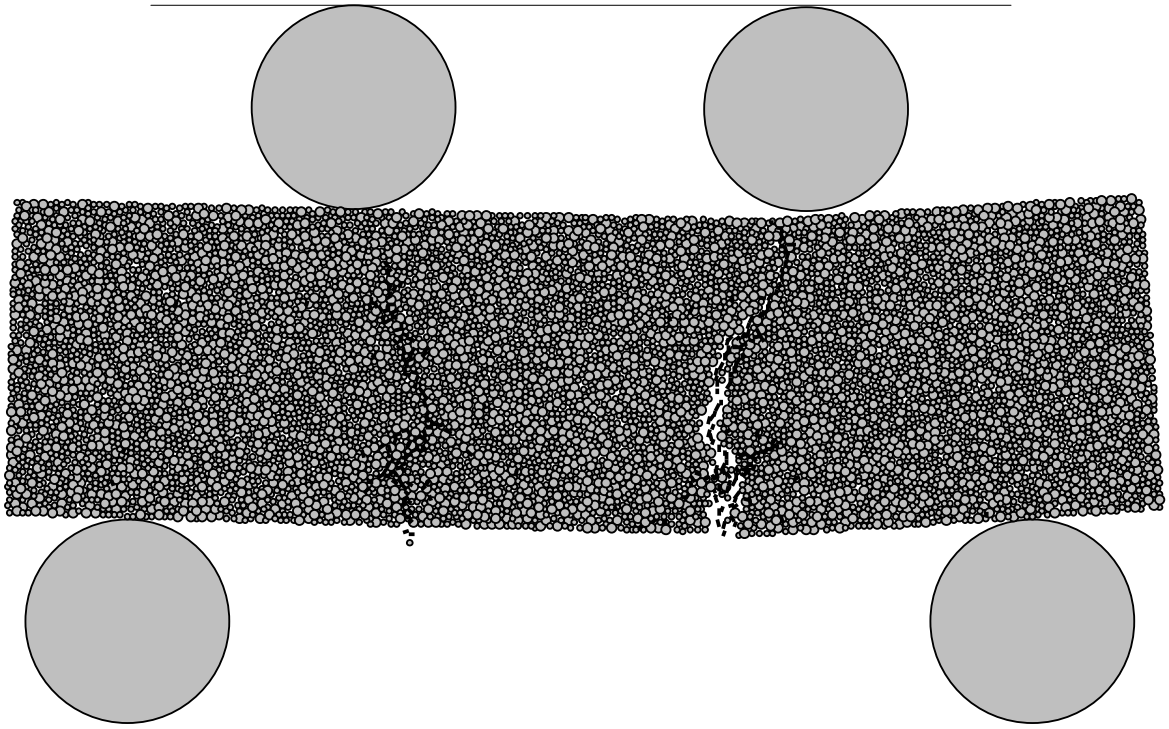

Figure 5.3: The fracture phenomenon in the sample with no defects.

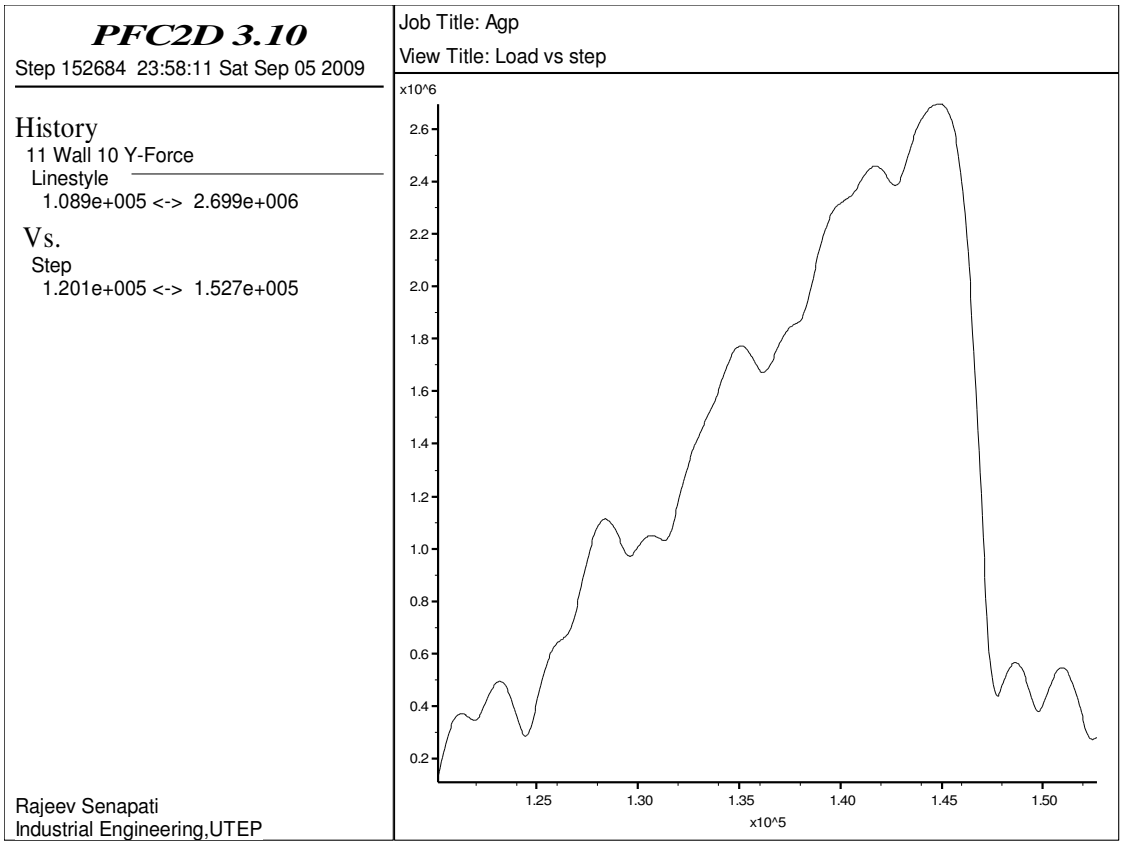

Figure 5.4: The force diagram of four-point bending test on the sample with no defects.

5.2.2 Sample With Material-Inherent Defect (void)

Four-Point bending test was performed on a sample with material-inherent defect. To simulate this, a sample with a void of radius 0.3 mm was created as shown in Figure 5.5.

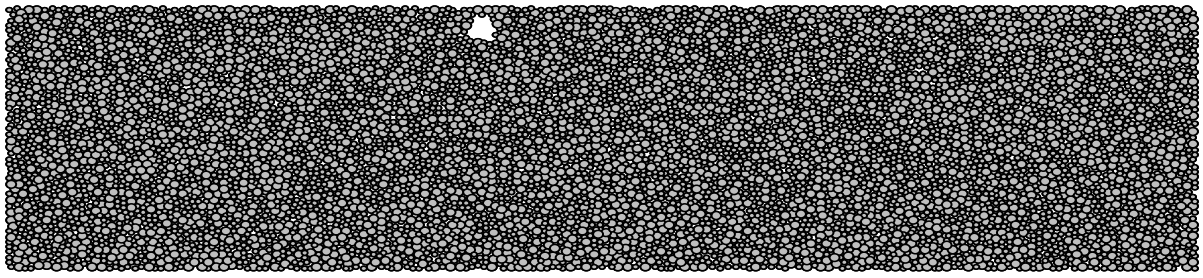

Figure 5.5: A silicon-nitride ceramic sample with a void generated using PFC^{2D}.

Figure 5.6 shows the simulation modeling of the samples with material-inherent flaws and the fracture of the sample by four-point bending test and Figure 5.7 shows the corresponding force diagram.

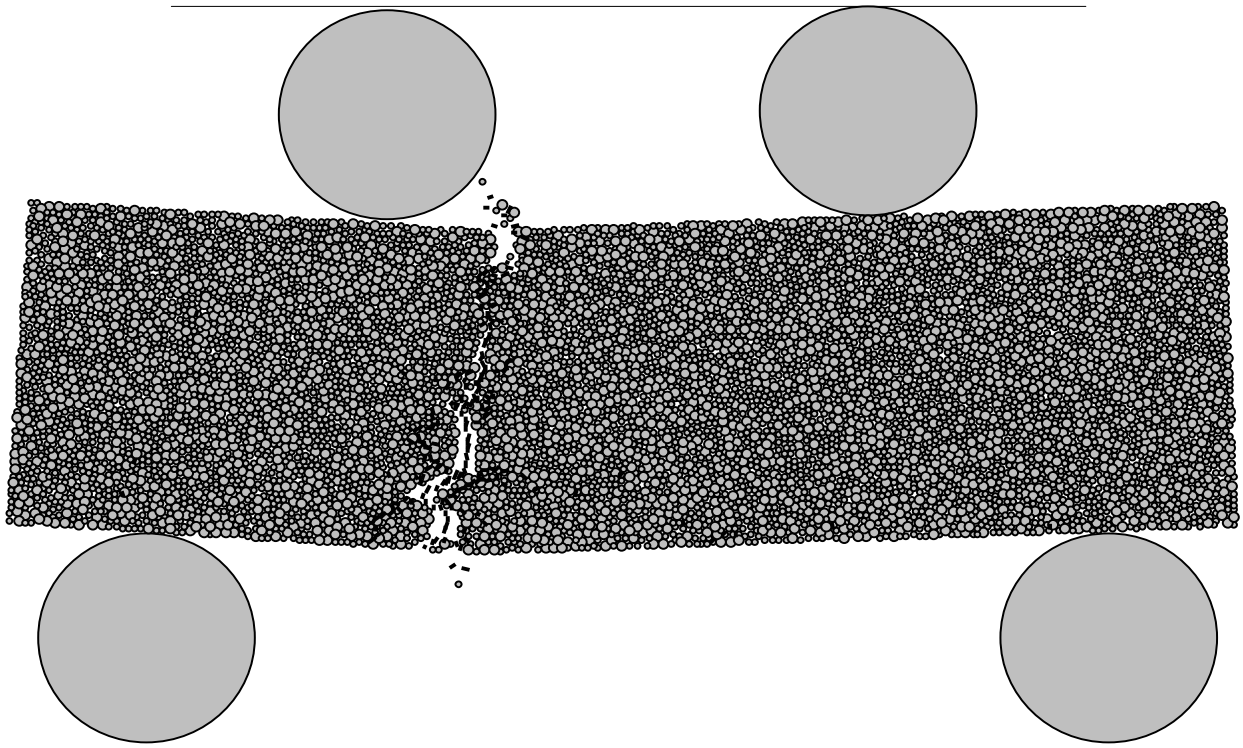

Figure 5.6: the fracture on the sample with void.

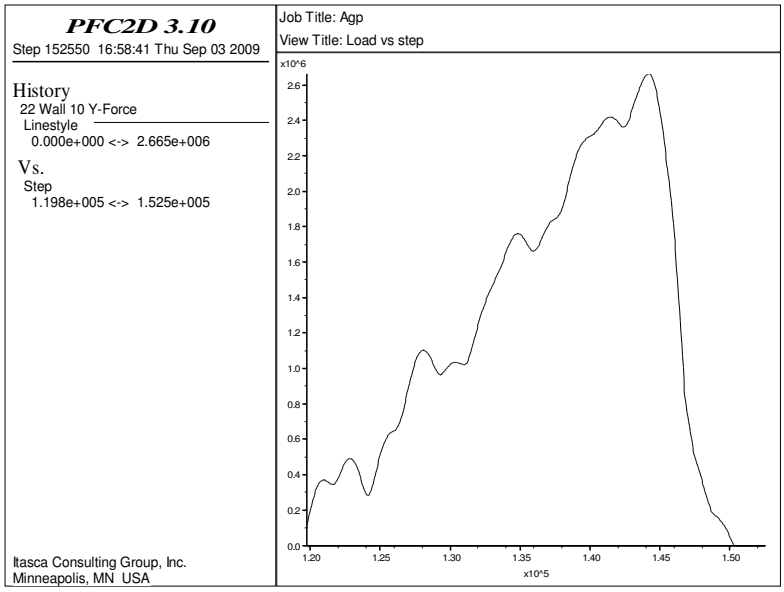

Figure 5.7: The force diagram of four-point bending test on the sample with material-inherent defects.

5.2.3 Sample With Manufacturing-Induced Defects (Cracks)

In this part, four-point bending test has been performed on a sample with manufacturing-induced defects. Figure 5.8 shows a sample of silicon-nitride ceramic generated by PFC^{2D} which has some initial cracks which are assumed to have been formed due to some manufacturing process. The simulation of the four-point bending test is shown in Figure 5.9, and Figure 5.10 shows the corresponding force diagram.

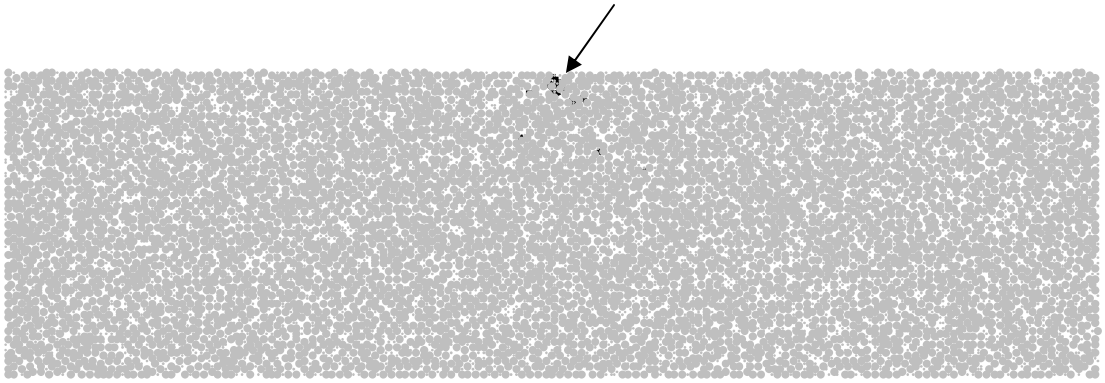

Figure 5.8: A silicon-nitride ceramic sample with cracks generated using PFC^{2D}.

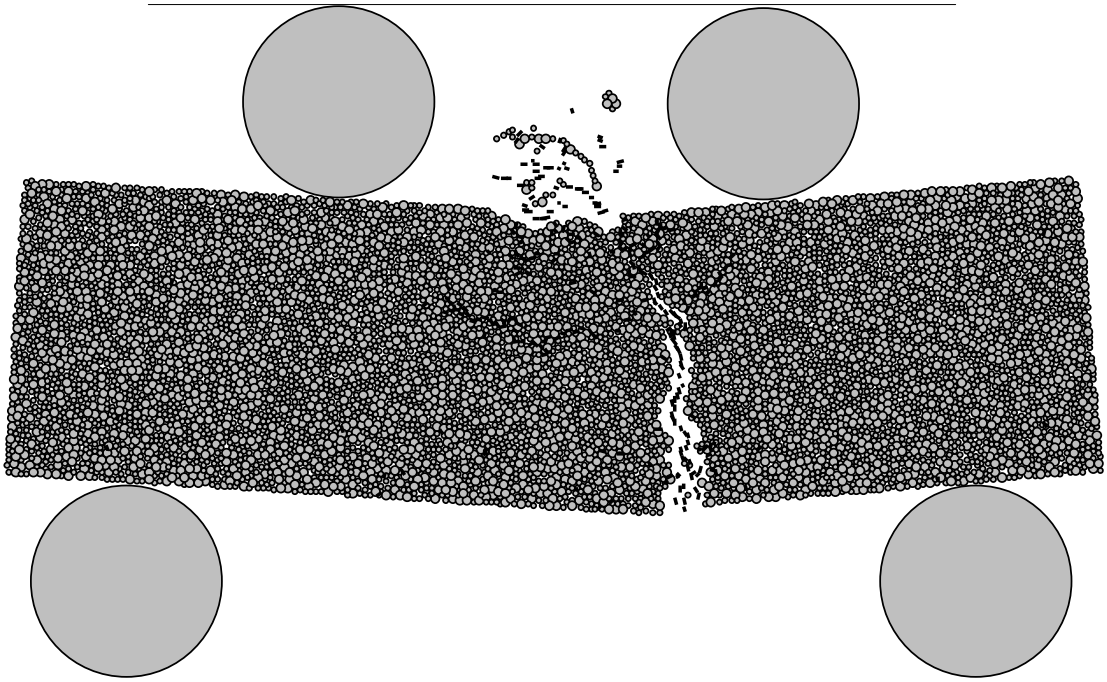

Figure 5.9: the fracture on the sample with initial cracks.

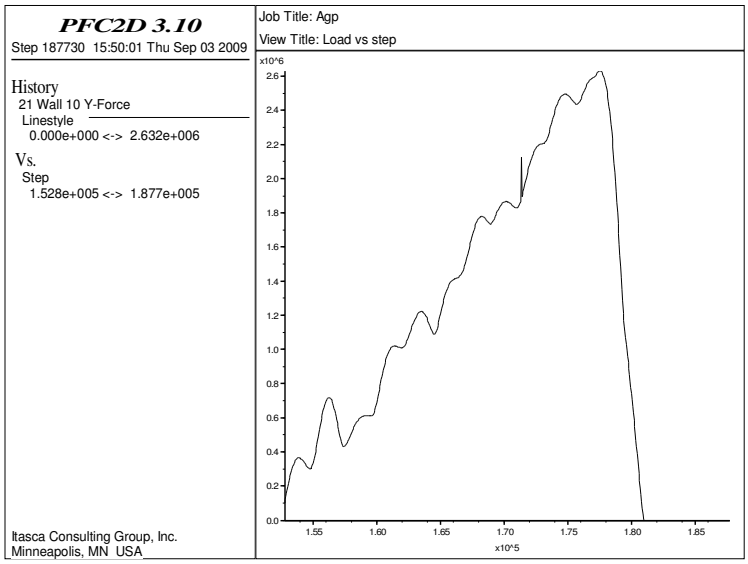

Figure 5.10: The force diagram of four-point bending test on the sample with manufacturing-inherent defects.

Chapter 6: Discussion

PFC^{2D} software package was used to simulate the Indentation Test and the Four – Point Bending Test which are difficult to perform experimentally in small samples and it is also not feasible to do it experimentally. In the Indentation test the sub – surface damage was simulated and also the applied force studied for three different cases. The crack formation in the sample due to indentation test is studied and it is seen that for a larger applied force the depth and width of the cracks formed are more.

6.1 Indentation Test

In the simulation of indentation test a DEM model of silicon nitride ceramic is created and the indentation test is performed on the sample for three different forces. The depth and width of the cracks formed are studied and are compared for different forces. The results obtained from PFC^{2D} are well in accordance with the experimental result. Figure 6.1 [44] shows the cracks formed in three different samples when they are subjected to three different loads in indentation test, the figure shows the Nomarski optical micrographs of the samples.

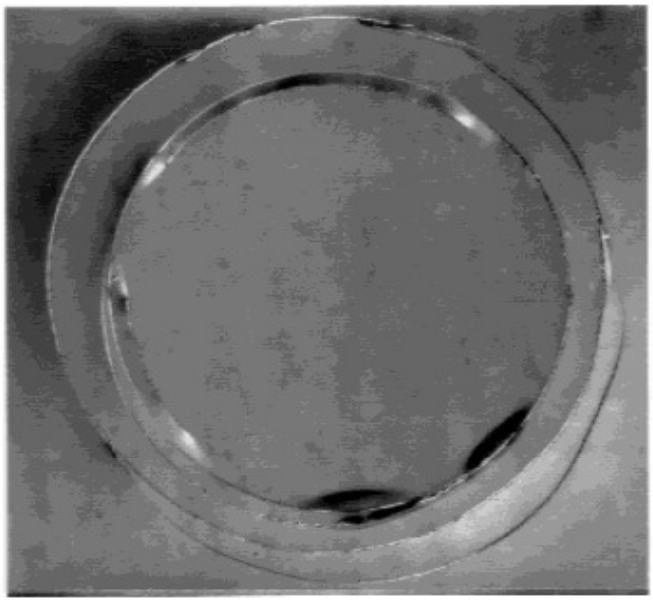

(a)

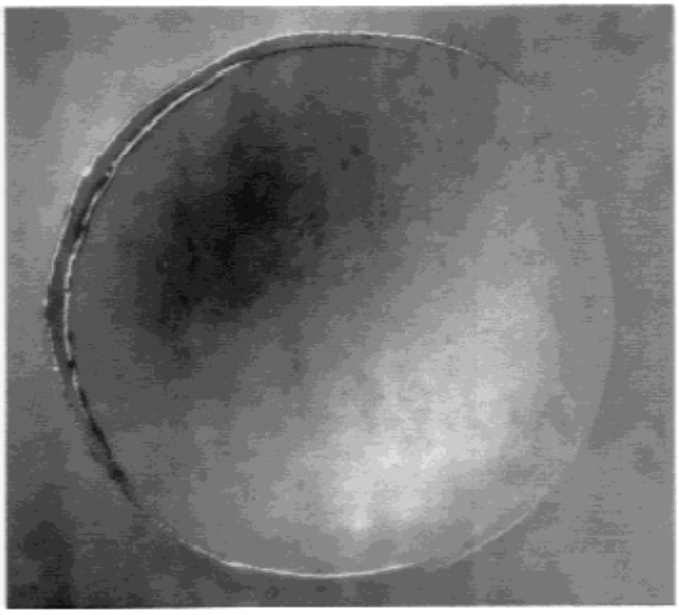

(b)

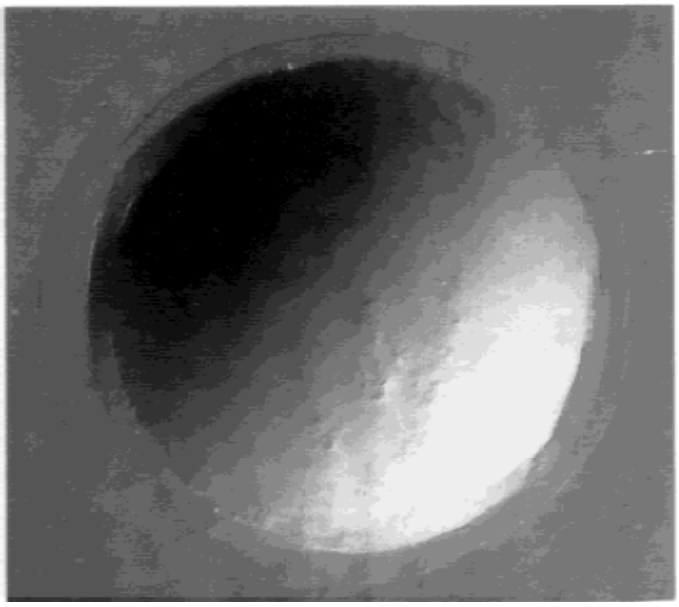

(c)

Figure 6.1: Cracks formed with loads (a) 2000 N, (b) 3000 N and (c) 4000 N.

From the above figures it is observed that the more the applied force, the more is the depth and width of the cracks formed in indentation test.

6.2 Four – point bending test

In the four – point bending test the applied force was studied and the force at which the sample fails was recorded for three different cases. The samples used for the test were a sample with no defects, a sample with material inherent defect like void and a sample with machining induced defects like cracks. After performance of the four – point bending test on these three samples it was observed that the sample with no defect required the maximum amount of force to fail. The point of crack initiation was also affected by the presence of any defects. The above results obtained by PFC^{2D} are well in accordance to the results obtained by Laser scattering. Figure 6.2 shows the fracture origin in the laser scattering images and Figure 6.3 shows the fracture strength of the sample. The images received by laser scattering shows that the fracture origin and fracture strength is highly influenced by the presence of material inherent flaws or machining induced flaws and the samples are fractured at the point of defect [45].

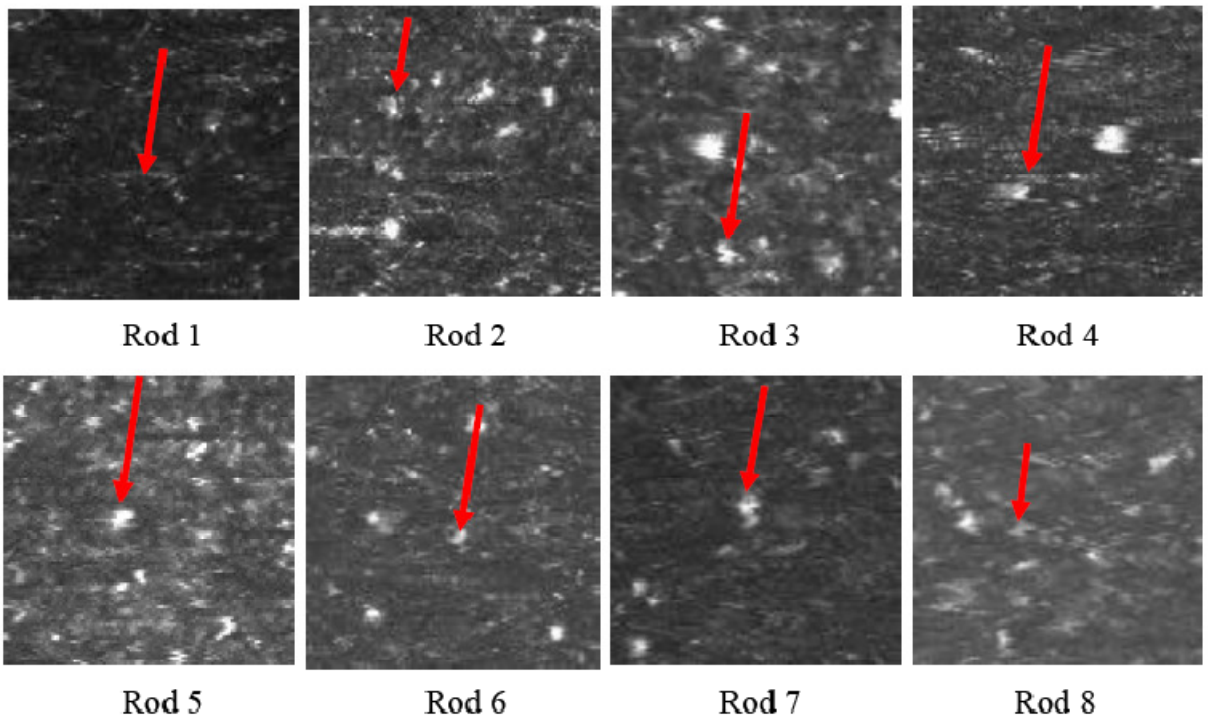

Figure 6.2: Fracture origins in laser scattering images.

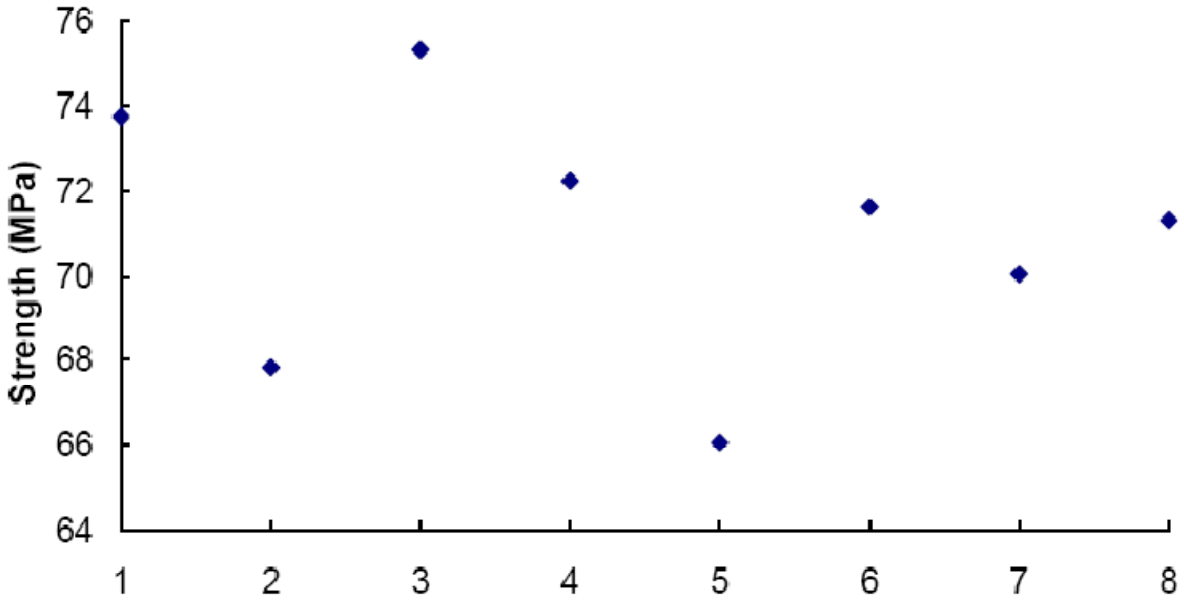

Figure 6.3: Fracture strength for the samples.

Chapter 7: Conclusion and Contributions

From the results obtained by the simulation of the Indentation test it is observed that the depth and width of the cracks formed in the Indentation test depends on the applied force, as the force is increased the depth and width of the cracks increases. The results obtained from the simulation of the Indentation test are well in accordance with the experimental results.

From the results obtained by the simulation of the four-point bending test it is observed that the sample with no pre-existing defect requires the maximum amount of force to fail. And the point of crack initiation is also affected by the presence of any kind of defect. The results obtained are well in accordance with the experimental results.

PFC^{2D} was initially used for the analysis of discontinuous media like rocks and soil mechanics, but recently its application is being explored for continuous media like ceramics. In future PFC^{2D} can be used for more continuous media and for different machining processes for the analysis of fracture. It can be also used to study the behaviour of other non – metals under different kind of loading or different machining processes. If the software is developed to an extent where we can simulate and study the results of actual destructive testing methods then the need for expensive laboratory setups to determine the behaviour of ceramic materials under loading can be eliminated. Further this software can be utilized to understand the behaviour of non homogeneous material like ceramic when stressed which may be helpful in understanding fracture mechanics better.

References

1. Sanchez,E., Miranda,P., Fernando, G. and Antonia, P., Effect of temperature on pre creep mechanical properties of silicon nitride, *Journal of the European Ceramic Society.* **29,** 2635 – 2641, (2009).
2. Andersson, P. and Lintula, P., Load-carrying capability of water-lubricated ceramic journal bearings, *Tribiology International,* **27**, 315 – 321 (1994).
3. Parker, K., Advanced Ceramics Soar to New Heights**,** *Metal Finishing,* **104,** 16 – 18 (2006).
4. Kitajima, K., Cai, G. Q. and Kumagai, N., Study on mechanism of ceramics grinding. *Annals of the CIRP*, **41**, 367–371, (1992).
5. Malkin, S. and Hwang, T. W., Grinding Mechanisms for Ceramics, *CIRP Annals – Manufacturing Technology,* **45,** 569 – 580 (1996).
6. Huang, H. and Liu, Y. C., Experimental investigations of machining characteristics and removal mechanisms of advanced ceramics in high speed deep grinding. *International Journal of Machine Tools & Manufacture*, **43**, 811–823, (2003).
7. Desa, O. and Bahadur, S., Material removal and subsurface damage studies in dry and lubricated single-point scratch tests on alumina and silicon nitride. *Wear*, **225–229**, 1264–1275. (1999).
8. Zhang, Z., Zhang, L. and Yiu-Wing, M., Modelling friction and wear of scratching ceramic particle-reinforced metal composites, *Wear,* **176,** 231 – 237 (1994).
9. Wataru, K., Subsurface damage in scratch testing of silicon nitride. *Wear*, **256**, 100–107, (2004).
10. Patten, J. A., Gao, W. and Yasuto, K., Ductile regime nanomachining of single-crystal silicon carbide. *ASME Journal of Manufacturing Science and Engineering*, **127**(8), 522–532, (2005).
11. Jasinevicius, R. G., Influence of cutting conditions scaling in the machining of semiconductors crystals with single point diamond tool. *Journal of Materials Processing Technology,* **179**, 111–116, (2006).
12. Martinho, R.P., Silva, F.J.G and Baptista, A.P.M, Wear behaviour of uncoated and diamond coated Si_3N_4 tools under severe turning conditions, *Wear,* **263,** 1417 – 1422 (2007).
13. Zhang, B. and Peng, X. H., Grinding damage prediction for ceramics via CDM model, Journal of Manufacturing Science and Engineering. *Transactions of the ASME,* **122**, 51–58, (2000).
14. Chuang, T. J., Jahanmir, S. and Tang, H. C., Finite element simulation of straight plunge grinding for advanced ceramics. *Journal of the European Ceramic Society,* **23**, 1723–1733, (2003).

15. Itasca Consulting Group Inc., Particle Flow Code in 2-Dimensions (PFC2D), Version 3.10, Minneapolis, Minnesota, 2004.

16. Gong, J., Wang, J. and Guan, Z. A comparison between Knoop and Vickers hardness of silicon nitride ceramics, *Materials Letters*, **56**, 941– 944, (2002).

17. Westman, A. K., Swain M. V., Bell, T. J. and Bendeli, A., Ultra-Micro Indentation Technique used for Examination of Mechanical Properties Close to an HIPed Surface of Silicon Nitride, *Journal of the European Ceramic Society*, **8**, 879-890, (1998).

18. Rani, D. A., Sakaguchi, S. Hirao, K., Yamauchi, Y. and Kanzaki, S., Estimation of Surface Stress from Sliding Scratch and Static Sphere Indentation, *Journal of Ceramic Society of Japan*, **111**, 294 – 299, (2003)

19. Jayaraman, S., Hahn, G. T., Oliver, W. C. and Rubin, C. A., Determination Of Monotonic Stress – Strain Curve of Hard Materials Ultra – Low – Load Indentation Tests, *International Journal of Solids Structures*, **35**, 365 – 381, (1998).

20. Rodrigues, S. A., Ferracane, J. L. and Bona, A. D., Flexural strength and Weibull analysis of a microhybrid Flexural strength and Weibull analysis of a microhybrid 4-point bending tests, *Dental materials*, **24,** 426 – 431, (2008).

21. Fischer, J., Stawarczyk, B. and Hammerle, C.H.F., Flexural strength of veneering ceramics for zirconia, *Journal of Dentistry*, **3 6**, 316 – 321, (2008).

22. Mujika, F., On the difference between flexural moduli obtained by three-point and four-point bending tests. *Polymer Testing,* **25**, 214–220, (2006).

23. Carneiro, J.O., Alpuim, J.P. and Teixeira, V., Experimental bending tests and numerical approach to determine the fracture mechanical properties of thin ceramic coatings deposited by magnetron sputtering, *Surface & Coatings Technology,* **200**, 2744– 2752, (2006).

24. D.O. Potyondy, P.A. Cundall, "A bonded-particle model for rock". International Journal of Rock Mechanics & Mining Sciences. 41:1329–1364, 2004.

25. Fakhimi, A., Carvalhoc, F., Ishidad, T., and Labuz, J.F., Simulation of failure around a circular opening in rock, *International Journal of Rock Mechanics & Mining Sciences,* **39**, 507–515, (2002)

26. Wang, C., Tannanta, D.D., and Lilly, P.A., Numerical analysis of the stability of heavily jointed rock slopes using PFC2D, *International Journal of Rock Mechanics & Mining Sciences* **40,** 415–424 (2003).

27. An, B. and Tannant, D. D., Discrete element method contact model for dynamic simulation of inelastic rock impact, *Computers & Geosciences,* **33**, 513–521, (2007).

28. Emeriault, F. and Claquin, C., Statistical homogenization for assemblies of elliptical grains: effect of the aspect ratio and particle orientation, *International Journal of Solids and Structures* **41,** 5837–5849 (2004).

29. Zhang, R. and Li, J., Simulation on mechanical behavior of cohesive soil by Distinct Element Method, *Journal of Terramechanics,* **43**, 303–316, (2006).

30. Shmulevich, I., Asaf, Z. and Rubinstein, D., Interaction between soil and a wide cutting blade using the discrete element method, *Soil & Tillage Research,* **97**, 37–50, (2007).

31. Moon, T., Nakagawa, M. and Berger, J., Measurement of fracture toughness using the distinct element method, *International Journal of Rock Mechanics & Mining Sciences,* **44,** 449–456, (2007).

32. Azevedo, N. M, Lemos, J.V., Hybrid discrete element/finite element method for fracture analysis, *Computer Methods in Applied Mechanics and Engineering*, **195**, 4579–4593, (2006).

33. Tan, Y., Yang, D. and Sheng, Y., Discrete element method (DEM) modeling of fracture and damage in the machining process of polycrystalline SiC, *Journal of the European Ceramic Society*, **29**, 1029–1037, (2009).

34. Wanne, T.S. and Young, R.P., Bonded-particle modeling of thermally fractured granite, *International Journal of Rock Mechanics & Mining Sciences,* **45**, 789–799, (2008).

35. Itasca Consulting Group Inc., *PFC^{2D} User's Manuals*, 2004.

36. Shan, S., Jia, Q., Jiang, L., Wang, Y. and Yang, J., Microstructure control and mechanical properties of porous silicon nitride ceramics, *Ceramics International*, **35**, 3371–3374, (2009).

37. Riley, F. L., Silicon Nitride and Related Materials, *Journal of the American Ceramic Society,* **83**, 245 – 265, (2000).

38. Buljan, S. T. and Baldoni, J. G. Silicon – nitride based composites, *Materials Science Forum,* **47**, 249 – 266, (1989).

39. Bal, B. S., Khandkar, A., Lakshminarayanan, R., Clarke, I., Hoffman, A. A. and Rahaman, M. N., Fabrication and Testing of Silicon Nitride Bearings in Total Hip Arthroplasty, *The Journal of Arthroplasty,* **24**, 110 – 116, (2009).

40. Petzow G, Herrmann M. Struct Bond (2002);102:47.

41. Dressler W, Kleebe HJ, Hoffmann MJ, Rouhle M, Petzow G. J (1996). European Ceramic Society (1996); 16:3.

42. Imamura H, Hirao K, Brito ME, Toriyama M, Kanzaki S (2000). J Am Ceram Soc 83:495

43. Yang, B., Jiao, Y. and Lei, S. A study of the effects of microparameters on macroproperties for the specimens created by bonded particles. *Engineering Computations: International Journal for Computer – Aided Engineering and Software.* **23**, 607 – 631, (2006).

44. Lee, S. K., Wuttiphan, S. and Lawn, B. R., Role of microstrusture in Hertzian contact damage in silicon nitride: I, mechanical characterization, *Journal of American Ceramic Society*, **80**, 2367 – 2381, (1997).

45. Zhang, J. M., Sun, J. G., Andrews, M. J., Ramesh, A., Tretheway, J. S. and Longanbach, D. M., Characterization of Subsurface defects in Ceramics Rods by Laser Scattering and Fractography, *American Institute of Physics Conference Proceedings on Quantitative Nondestructive Evaluation,* **820**, 1209 – 1216, (2006).

Appendix – A

Indentation Test

1. Code to generate the sample:

```
; Filename: Agp.DVR
;
; ================================================================
new
set safe_conversion on
set random=1200 ; for reproducibility
set disk on ; model unit-thickness cylinders
;SET logfile cluster.log
;set log on
;
set gen_error off
SET echo off ; load support functions
call md_bending.FIS
call et2.FIS
call flt.FIS
call cluster.FIS
SET echo on
; ================================================================
SET md_run_name = 'Agp'
title
Agp (material-A, gross resolution, parallel-bonded)
; ================================================================

; Specify parameters that control the specimen-genesis procedures
;
SET et2_xlen=20.0e-3 et2_ylen=7.0e-3
SET et2_radius_ratio=2.0 et2_rlo=0.5e-4
;Set et2_rlo=0.6e-3
```

```
SET md_wEcfac=5.0

SET tm_req_isostr=-1.0e7 tm_req_isostr_tol=0.50

SET flt_def=3 flt_remain=0.0


; Specify parameters that define a parallel-bonded material

SET md_add_pbonds=1

SET md_dens=3200.0

SET md_Ec=220e9 md_knoverks=1.3

SET pb_radmult=1.0 pb_Ec=220e9 pb_knoverks=1.3

SET md_fric=0.4

SET pb_sn_mean_btn=1600e6 pb_sn_sdev_btn=400e6   ; initially mean = 1400, std
dev = 280

SET pb_ss_mean_btn=3200e6 pb_ss_sdev_btn=800e6   ; initially mean = 1400, std
dev = 280

;

set tm_steps=100000

;  ------- for clusters

SET md_clusters=1

SET pb_sn_mean=1e30 pb_sn_sdev=0.0

SET pb_ss_mean=1e30 pb_ss_sdev=0.0


SET EXTRA ball 3

SET cl_size=3

SET cl_bslt=1


; ---------------- ----------

SET et2_prep_saveall=1

et2_prep ; invoke the specimen-genesis procedures

;call indentation.txt

; ====================================================================

return

; END OF Filename: Agp.DVR
```

2. Code for the Indentation test

```
;fname: Indentation.DVR  (Programm for Indentation test)
;
new
restore Agp-spc.sav
;
SET echo off   ; load support functions
  call %itascaFishTank%\FishPfc\md\fishcall.FIS
  call %itascaFishTank%\FishPfc\md\crk.FIS
crk_init
delete wall 2
;solve
;
; ================================================================
def loadball
  x1=et2_xlen/4
  x2=-x1
  y1=et2_ylen/2 + brad
  y2= -y1
  x6=et2_xlen
  y3=-et2_ylen
  x5=x3/4
  x4=-x5
  x3=-x6
  x10=-2*brad
  y10=y1+brad
  x11=-x10
```

```
  y11=y10
 command
    ball rad=brad id=19507 x=0 y=y1
    wall id 10 nodes (x11,y11) (x10,y10)
    ;wall id 11 nodes (x3,y3) (x4,y3)
    ;wall id 12 nodes (x5,y3) (x6,y3)
 end_command
 command
  prop dens=3200.0 kn=1e11 ks=1e11 fric=0.0 range id=19507
  wall id 10 ks 1e11 kn 1e11 fric 0.0
  ;wall id 11 ks 1e11 kn 1e11 fric 0.0
  ;wall id 12 ks 1e11 kn 1e11 fric 0.0
 end_command
end
; ===================================================================
def acc_wall
;
; ----- Accelerate the wall in controlled fashion to achieve
;       final velocity of [w_vel] over approximately [w_cyc] cycles
;       in [w_stages] stages.
;
; INPUT:  vel_w    - final platen velocity    (float)
;         cyc_w    - total number of cycles   (integer)
;         stages_w - number of intervals      (integer)
;
  dv_w = vel_w / stages_w
  niter_w = cyc_w / stages_w
```

```
  vel_w = 0.0
    loop ap_ii (1,stages_w)
    vel_w = vel_w + dv_w
    fvel_w = vel_w
    command
      wall id=10  yvel= vel_w
      cycle niter_w
    end_command
   end_loop
end
; ====================================================================



set brad=2.25e-3   ; 1.98


loadball
fix x range id= 19507
property xvel=0  range id= 19507
;fix y ra id=19506 19505
;property yvel=0 ra id= 19506 19505
free spin ra id= 19507
set vel_w=-2.0     ; 2.0
SET  cyc_w=400  stages_w=10
acc_wall
history id=20 diagnostic mcf id 19507
hist id 11 wall yforce id 10
;plot create figure_cluster
```

```
plot add ball

plot add wall

plot add cluster ac on id on

;plot add velocity red

;plot add fish flt_item

;plot add fish crk_item

;plot show


SET md_run_name = 'Crack'

title

Crack


plot create figure_crack

;plot add ball

plot add wall

plot add fish crk_item black

plot show


SET md_run_name = 'Load'

title

Focre on the laoding ball

plot create Force_on_loading_ball

;plot add wall

;plot add ball

plot add hist 11

;plot add hist 20

plot show
```

```
cyc 35000

save Indentation1.SAV

;

return
```

Appendix – B

Four – point bending test

1. Code to generate the sample with no defects.

```
; Filename: Agp.DVR
;
; <comments removed. . .>
; ================================================================
new
set safe_conversion on
SET random=10000 ; for reproducibility
SET disk on ; model unit-thickness cylinders
;SET logfile cluster.log
;set log on
;
SET echo off ; load support functions
call md_bending.FIS
call et2.FIS
call flt.FIS
call cluster.FIS
SET echo on
; ================================================================
SET md_run_name = 'Agp'
title Agp (material-A, gross resolution, parallel-bonded)
; ================================================================
; Specify parameters that control the specimen-genesis procedures
;
SET et2_xlen=25.0e-3 et2_ylen=7.0e-3
SET et2_radius_ratio=2.0 et2_rlo=0.5e-4
;Set et2_rlo=0.6e-3
;
;set et2_tunnel=1

SET md_wEcfac=5.0
SET tm_req_isostr=-1.0e7 tm_req_isostr_tol=0.50
SET flt_def=3 flt_remain=0.0
; Specify parameters that define a parallel-bonded material
;
SET md_add_pbonds=1
SET md_dens=3200.0
SET md_Ec=220e9 md_knoverks=1.3
SET pb_radmult=1.0 pb_Ec=220e9 pb_knoverks=1.3
SET md_fric=0.4
;SET pb_sn_mean_btn=1400e6 pb_sn_sdev_btn=280e6
SET pb_sn_mean_btn=1600e6 pb_sn_sdev_btn=400e6

;SET pb_ss_mean_btn=1400e6 pb_ss_sdev_btn=280e6
SET pb_ss_mean_btn=3200e6 pb_ss_sdev_btn=800e6
;
set tm_steps=100000

;  ------- for clusters
SET md_clusters=1
SET pb_sn_mean=1e30 pb_sn_sdev=0.0
SET pb_ss_mean=1e30 pb_ss_sdev=0.0

SET EXTRA ball 1
SET cl_size=15
```

```
SET cl_bslt=1
; ---------------- ----------
SET et2_prep_saveall=1
et2_prep ; invoke the specimen-genesis procedures

;call pbstrength.txt
;call c:\budong\cluster\stone\Brazilian.txt

;call c:\budong\cluster\stone\Compression.DVR
;call Bend4p.DVR

; ===================================================================
return
; END OF Filename: Agp.DVR
```

2. Code to generate the sample with material - inherent defect (void).

```
;fname: manufacturingdefect.DVR   (Programm for creating a sample having a
manufacturing defect)
;
new
restore Agp-spc.sav

delete wall 1
delete wall 2
delete wall 3
delete wall 4
;
SET echo off   ; load support functions
  ;call %itascaFishTank%\FishPfc\md\fishcall.FIS
  ;call %itascaFishTank%\FishPfc\md\crk.FIS

;crk_init

macro Hole 'circle center -2.5e-3 2.9e-3 rad 0.3e-3'
del ball range Hole

plot add wall
plot add ball
plot show

save Bend4p2.sav
```

3. Code to generate the sample with machining – induced defect (crack).

```
;fname: creatingsample.DVR  (creating sample with initial cracks)
;
new
restore Agp-spc.sav
;
SET echo off   ; load support functions
  call %itascaFishTank%\FishPfc\md\fishcall.FIS
  call %itascaFishTank%\FishPfc\md\crk.FIS
SET echo on
crk_init
;
;pause
;
;delete ball 1
;delete ball 2
;delete ball 3
;his reset
```

```
;delete wall 1
delete wall 2
;delete wall 3
;delete wall 4
solve
;
; ================================================================
def loadball
; generate support and loading balls
  y_low=-0.5*et2_ylen
  y_up=0.5*et2_ylen

  x1=-L_4p/3
  y1=y_low-brad
  x2=L_4p/3
  y2=y1
  x3=0
  y3=y_up+brad
  x4=L_4p/8
  y4=y3
  x10=x3-2*brad
  y10=y3+brad
  x11=x4+2*brad
  y11=y10
 command
  ;ball rad=@brad id=50001 x=@x1 y=@y1
  ;ball rad=@brad id=50002 x=@x2 y=@y2
  ball rad=@brad id=50003 x=@x3 y=@y3
 ; ball rad=@brad id=50004 x=@x4 y=@y4
  wall id 10 nodes (@x11,@y11) (@x10,@y10)
 endcommand
 command
  prop dens=3200.0 kn=1e11 ks=1e11 fric=0.0 ra id=50001,50004
  wall id 10 ks 1e11 kn 1e11 fric 0.0
 endcommand
end
; ====================================================================
def acc_wall
;
; ----- Accelerate the wall in controlled fashion to achieve
;       final velocity of [w_vel] over approximately [w_cyc] cycles
;       in [w_stages] stages.
;
; INPUT:  vel_w    - final platen velocity    (float)
;         cyc_w    - total number of cycles   (integer)
;         stages_w - number of intervals      (integer)
;
  dv_w = vel_w / stages_w
  niter_w = cyc_w / stages_w
  vel_w = 0.0
  loop ap_ii (1,stages_w)
    vel_w = vel_w + dv_w
;    fvel_w = vel_w
    command
      wall id=10  yvel= @vel_w
      cycle @niter_w
    end_command
  end_loop
end
; ====================================================================
def deflection
  wid=10
  wp=find_wall(wid)
  deflection=w_y(wp)
```

```
end
;=========================================================================
;
set brad=2.25e-3
set L_4p=et2_xlen ;L1_4p=20e-3
;set L_4p=22.86e-3 L1_4p=10.16e-3   ;based on Smith and Quackenbush
;set D_4p=6.35e-3 b_4p=2.59e-3 h_4p=1.27e-3 ;Smith and Quackenbush
loadball
plot create crack
;plot mod ball id=1 yellow
;plot add ball
plot add wall
plot add fish crk_item
;plot add cluster ac on id on
plot show
;plot add vel red
;
fix x range id=50001,50004
property xvel=0 range id=50001,50004
fix y range id=50001,50002
property yvel=0 range id=50001,50002
free spin range id=50001,50004
;
;set vel_w=-0.0083e-3 ; This is the ASTM standard speed (5mm/min)
set vel_w=-2.0
SET  cyc_w=400  stages_w=10
acc_wall
;
;wall id 10 yvel -0.2e-3
;prop s_bond=5e5 n_bond=5e5
hist id 11 wall yforce id 10
hist id 12 deflection
set display his 11  ; add hist-11 to the status report while cycling
set display his 12
;
plot create Load
plot add hist 11
plot set title text 'Load vs step'
;plot show
;
plot create Displacement
plot add hist 12
plot set title text 'Displacement vs step'
;plot show
;
cyc 35500
save bend4p1.SAV
;
return
; ============================================================
;EOF: bend4p.DVR
```

Curriculum Vitae

Rajeev Senapati son of Mr. S. N Senapati and Mrs. L. Senapati was born and brought up in India. He received his bachelor's degree in Mechanical Engineering from Rashtrasant Tukadoji Maharaj Nagpur University, India. He joined University of Texas at El Paso (UTEP) to pursue graduate studies in Engineering. While his course of stay at UTEP as master's student he worked as a Research Assistant under the supervision of Dr. Jianmei Zhang, who is an expert in the area of detection of cracks using the non destructive techniques. He attended the Quantitative Non – Destructive Evaluation 2009 conference held in University of Rhode Island, Kinston, RI and presented his work on Identifying Fracture Origin in Ceramics by Combination of Nondestructive Testing and Discrete Element Analysis.

Address: 4111 Westcity CT

Apt # 220

El Paso, TX, 79902

This thesis was typed by Rajeev Senapati.